Molecular complexes of 4, 4'-dinitrobiphenyl

by

Binnur Tuncel van Pomeren

Submitted in fulfilment of the requirements for the degree of

Master of Science in Chemistry

In the Faculty of Natural and Agricultural Sciences

University of Pretoria

Pretoria

July 2004

CONTENT

Acknowledgement

I would like to thank Prof. P.H. van Rooyen for his continuous feedback throughout the study. This helped me to understand the background of many principles in both chemistry and physics in a broader perspective than I previously had.

Prof. R. Vleggaar was indispensable in developing my skills for synthetic methods and for questioning what may have occurred to the organic compounds covered in this study.

Mrs. L. Prinsloo put in a great effort to assist me with the interpretation of the results of infrared and Raman studies on the compounds of this study. Her deep knowledge of these methods gave me a secure feeling that the conclusions drawn from the study were scientifically based.

Prof. F.D. Auret, Department of Physics, helped me with the analysis of these compounds to test for electrical conductivity in the solid state.

Dr. S. Verryn, Department of Geology, assisted me in obtaining and analysing the data from powder diffraction methods.

Prof. F.H. Herbstein proved to be a priceless source for developing new strategies for my study on π-interactions, thanks to his review book “Perspectives in Structural Chemistry”.

Thank you to all the people in the Chemistry Department for supporting me, either directly or indirectly during the study. This interaction helped me to keep the study going.

List of Abbreviations

4,4'-DiOHBP	4,4'-Dihydroxybiphenyl
4,4'-DNBP	4,4'-Dinitrobiphenyl
4-BrBP	4-Bromobiphenyl
4-OHBP	4-Hydroxybiphenyl
BP	Biphenyl
BZ	Benzidine
C-44DiOHBP	Complex of 4,4'-Dinitrobiphenyl with 4,4'-Dihydroxybiphenyl
C-4BrBP	Complex of 4,4'-Dinitrobiphenyl with 4-Bromobiphenyl
C-4OHBP	Complex of 4,4'-Dinitrobiphenyl with 4-Hydroxybiphenyl
C-BP	Complex of 4,4'-Dinitrobiphenyl with Biphenyl
C-BZ	Complex of 4,4'-Dinitrobiphenyl with Benzidine
C-tmethylbz11	Complex of 4,4'-Dinitrobiphenyl with [*N*, *N*, *N'*, *N'*]-tetramethylbenzidine (1:1)
C-tmethylbz41	Complex of 4,4'-Dinitrobiphenyl with [*N*, *N*, *N'*, *N'*]-tetramethylbenzidine (4:1)
DMF	*N*, *N*-Dimethylformamide
DMSO-d_6	deuteriated dimethylsulfoxide
DSC	Differential Scanning Calorimetry
IR	Infrared
K	Kelvin
NMR	Nuclear Magnetic Resonance
$PdCl_2(PhCN)_2$	Bis(benzonitrile)dichloropalladium(II)
RT	room temperature
TDAE	Tetrakis(dimethylamino)ethylene
TG	Thermogravimetry
tmethylbz	[*N'*, *N'*, *N'*, *N'*]-tetramethylbenzidine

List of Compounds

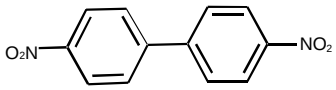

4,4'-Dinitrobiphenyl
$C_{12}H_8N_2O_4$
MW 244.21 g/mol

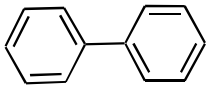

Biphenyl
$C_{12}H_{10}$
MW 154.21 g/mol

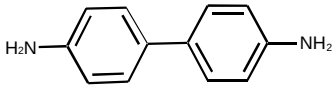

Benzidine
$C_{12}H_{12}N_2$
MW 184.2 g/mol

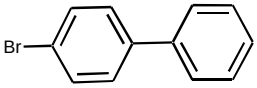

4-Bromobiphenyl
$C_{12}H_9Br$
MW 233.11 g/mol

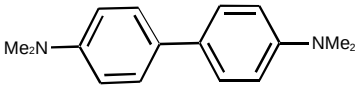

[N', N', N']-tetramethylbenzidine
$C_{16}H_{20}N_2$
MW 240.35 g/mol

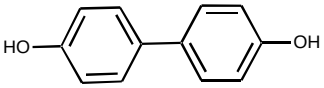

4,4'-Dihydroxybiphenyl
$C_{12}H_{10}O_2$
MW 186.21 g/mol

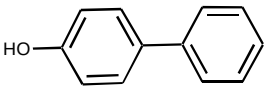

4-Hydroxybiphenyl
$C_{12}H_{10}O$
MW 170.21 g/mol

Summary

This study attempted to correlate the chemical and physical properties of the *para* disubstituted and *para* monosubstituted biphenyl complexes of 4,4'-DNBP with their structural and electronic properties, using a variety of physical and spectroscopic techniques, and X-ray diffraction methods. These complexes drew considerable attention in the past due to their capacity to demonstrate intense colours from yellow to dark red, which are dissimilar to the colour combination of their parent compounds. This prompted a series of investigations in the past through which the full structure of only Complex of 4,4'-Dinitrobiphenyl with 4-Hydroxybiphenyl (C-4OHBP) by single crystal diffraction was determined and the infrared and Raman spectra of C-4OHBP, Complex of 4,4'-Dinitrobiphenyl with Biphenyl (C-BP) and Complex of 4,4'-Dinitrobiphenyl with 4-Bromobiphenyl (C-BrBP) were obtained. In this study, other *para*-disubstituted biphenyl complexes with 4,4'-DNBP were investigated to add to the existing knowledge base and to study the effects of varying the substitution on the aromatic rings of the donor.

Because the complete solid state structures of the complexes in this study (except C-4OHBP) and the donor compound BZ are not known, their single crystal determination was attempted. Unfortunately, no suitable diffraction quality crystals could be crystallised. Although the X-ray crystal structure of 4,4'-DNBP was determined by photographic methods by Van Niekerk and Boonstra, the R-factor of this solution was relatively high at 15%, which is outside the current internationally accepted standard. Because the current technology using automated diffractometers is superior to photographic techniques used by Van Niekerk and Boonstra, it was decided to repeat the crystallographic analysis for 4,4'-DNBP. However, despite repeated efforts with a large variety of solvents used during the crystallisation process in this study, the crystals formed were of a relatively poor quality, resulting in a solution with a final R-factor of also only 15%.

Therefore, the only crystallographic data available for correlation with the physical properties of the complexes have been that of the uncomplexed compounds (except BZ) and C-4OHBP from

the previous studies. Based on these results, the comparison of the dihedral angles between the two aromatic rings of the parent compounds with their infrared and Raman spectra yielded that, unlike the conventional compounds the centrosymmetricity of the biphenyl derivatives cannot be uniquely determined by their infrared and Raman spectra.

Using thermogravimetric measurements, melting points and phase transitions of each pure component and as well as the complexes were obtained. Packing energy in the complex seems to be relatively more favourable than in the parent components alone. Otherwise, two phase transitions could be expected, one resulting from 4,4'-DNBP and one resulting from the other component in the complex.

Complex of 4,4'-Dinitrobiphenyl with 4,4'-Dihydroxybiphenyl (C-44DiOHBP) and Complex of 4,4'-Dinitrobiphenyl with Benzidine (C-BZ) showed some unexpected high melting points in their thermogravimetric studies. These elevated melting points are interpreted as resulting from hydrogen bonding, and infrared studies of these complexes confirmed this interpretation.

Conductivity measurements in the solid state revealed that only tmethylbz exhibits a measure of charge transfer. The absence of current in both its complexes (1:1 and 1:4 ratio) with 4,4'-DNBP was attributed to the close-packing and twisting of the components in the complex which prevented the electron flow through the complexes.

Because ultraviolet-visible, infrared and Raman spectra showed only small shifts in the pure compounds after complexation in solution, and their conductivity measurements revealed no current flow, the interactions in those complexes are ascribed mainly to Van der Waals forces.

The previously assigned moleular ratios are incorrect. This study has reassigned these molecular ratios using nuclear magnetic resonance techniques. Nuclear magnetic resonance spectroscopy detected only very small chemical shifts in the pure compounds after they formed complexes in solution. As these solutions did not maintain the colour of complexation, this could be seen as supportive proof that all the interactions involved in the formation of these complexes are very weak. The same conclusion as the previous studies has been reached, notably that the molecular

ratios, in which the components of these complexes unite, are caused almost exclusively by packing factors and are stabilised by weak interactions.

CHAPTER 1 Introduction

Properties of materials in the solid state and in solution, are influenced by the way molecules interact with one another. On the one hand there are the weak attractions (generally less than 4 kJ. mol^{-1}) of two closed-shell atoms, attributable to dispersion or Van der Waals interaction [1, 2], and on the other hand, the strong interaction of a chemical bond with a stabilisation of 209 kJ. mol^{-1} or more. Between these two limits there are various interactions of intermediate strength including electron donor-electron acceptor interactions present in complexes and hydrogen bonds.

The nature of such interactions in a complex is often complicated because different contributing terms of energy (*electrostatic, polarisation, exchange repulsion, charge transfer and coupling*) can make distinct contributions to the stabilisation [2]. These interactions are described as secondary interactions if they have no localised covalent bond formation within the interaction that leads to complex formation [3]. *Electrostatic interaction* can be either attractive or repulsive and is an interaction between the undistorted electron distribution of the contributing molecules. It differs from the *polarisation interaction* which is caused by distortion of the electron distribution of one compound by another [2]. In *exchange repulsion* the interaction is caused by exchange of electrons between the contributing compounds. This is a short-range repulsion due to overlap of electron distribution of one compound with that of the other compound [2]. *Charge transfer*, or *electron delocalisation*, involves the charge transfer from occupied molecular orbitals of one compound to vacant molecular orbitals of the other. For charge transfer to occur one component should have a higher electron affinity and the other component should have a low-ionisation potential. All these interactions can be calculated to some extent and help the prediction of the energetically favourable conformations of a molecule. However, there are some types of interactions for which the theoretical values cannot be calculated: these interactions are called *coupling* and account for higher order interaction between various components [2].

These weak interactions can give rise to the formation of hydrogen bonding which is weak in nature. Hydrogen bonding normally occurs between hydrogen atoms and neutral electronegative

atoms, such as N, O and F, and neutral proton donor groups such as F-H, O-H, N-H and C-H. This excludes ionic or strong hydrogen bonding which is of a very different nature [2].

In crystals containing bimolecular or multimolecular building blocks, these associative forces stabilise the molecular components in a highly ordered manner and result in the formation of molecular complexes. These forces are likely to make a high contribution to stabilising the formation of a molecular complex with a fixed stoichiometry. These forces are stronger than Van der Waals forces and stabilise crystal formation both compositionally and structurally with respect to each component [1, 3, 4].

Inclusion compounds such as clathrates contain a host lattice structure with void space-like cages in which a guest molecule can be incorporated without any other significant secondary interactions stabilising the complex. These crystals have a fixed structure with respect to the host but can vary with respect to the guest molecules. Not all void spaces have to be filled with guest molecules although there is usually a minimum concentration of the guest needed for the formation of the host lattice. This is unlike molecular complexes in the sense that they do not have a fixed stoichiometry requirement although there may be a minimum concentration of the guest needed for the formation of the host lattice [1].

Previously, some complexes of 4,4'-DNBP and 4-nitrobiphenyl were prepared, and some results were reported by Saunder, Van Niekerk and Boonstra [5, 6]. It was concluded that the ordered structures of these π-molecular complexes are governed primarily by geometrical factors and are stabilised by Van der Waals forces. Bolton and Prasad [1] confirmed this by their infrared and Raman results and considering that the molecular complexes of 4,4'-DNBP were obtained in fixed ratios, they concluded that these molecular complexes bridged the gap between the conventional complexes and inclusion compounds.

Another interesting feature of these complexes is intense colours which can vary from yellow to dark red, often completely unlike the colours of their parent compounds. The colours of both the parent compounds and their complexes with 4,4'-DNBP are shown in Table 1. The complexes of 4,4'-DNBP with BZ, with tmethylbz derivatives and with 4,4'-DiOHBP appear to be by far the

most intensely coloured. In previous studies all of these light coloured complexes melted with decomposition over approximately the same temperature range indicating that they were less stable than their more intensely coloured analogues [7].

Table 1 Some properties of parent compounds and molecular complexes

Parent compounds	Colour	Donor compounds	Colour	4,4'-DNBP: donor ratios from the literature [7]
4,4'-DNBP	light yellow			
BZ	brownish grey	C-BZ	bright red	4:1
tmethylbz	brownish yellow	C-tmethylbz11	blackish red	1:1
tmethylbz	brownish yellow	C-tmethylbz41	dark red	4:1
4-OHBP	white	C-4OHBP	light yellow	3:1
BP	white	C-BP	light yellow	3:1
4-BrBP	white	C-4BrBP	cream	3.5:1
4,4'-DiOHBP	white	C-44DiOHBP	bright yellow	3:1

The variation and intensity of these changes in colour have not been satisfactorily explained and could possibly be ascribed to charge transfer involving the complete transfer of an electron from donor to acceptor in the excited state [3] or to other structural or electronic factors such as the presence of auxochromes which cause a bathochromic shift in the absorption of the chromophores. Although examples of charge transfer in organic molecules exist, organic molecules have, in general, few strong electron acceptors and donors. For this reason, it is of interest to compare typical values of electron affinity (EA) and ionisation potentials (I) for organic donors and acceptors with those for alkali metal and halogen atoms: for a typical organic donor such as I=7 eV, for lithium iodide I=5.4 eV, for cesium iodide I=3.9 eV; for the best organic electron acceptor such as EA= 2 eV whereas for inorganic electron-acceptor fluorine EA= 3.4 eV [3]. π-Interactions are one of the most encountered forms of charge transfer (partial ionic formation) in the aromatic molecular complexes [3]. In organic molecules, substituents can enhance or diminish acceptor strength, depending on the type, number and location of [1, 3, 7]. Compounds with electron-withdrawing substituents, such as nitro-groups and halogens, display an increased ‘electron deficiency’ and will act as acceptors. The converse is true for donors: electron-donating substituents such as amine or alkyl groups make the donor more ‘electron-rich’ and increase the stability of the donor in the molecular complex. In this study the 4,4'-DNBP can therefore be classified as an acceptor, while BZ, tmethylbz, 4-OHBP, BP and 4-BrBP are donor molecules. For practical purposes this study will use this classification.

Some authors, on the other hand, consider π–π interaction as an interaction whose main components are Van der Waals and electrostatic forces rather than charge transfer [8, 9]. Hunter and Sanders use this model in the analysis of the geometrical arrangement of aromatic molecules [8]. The model works for a large variety of compounds, but suffers from a drawback in that it ignores the short-range effects (such as hydrogen bonding) and induction [8, 9]. The key feature of the model is that the σ framework and the π electrons are considered separately and that net σ-π interactions are actually the result of interactions that overcome π-π repulsions.

This study seeks to clarify which of these bonding properties exist in the molecular complexes of 4,4'-DNBP, by using the results from single crystal x-ray diffraction and spectroscopic studies.

1.1 Historical Background

1.1.1 Biphenyl and 4,4'-DNBP molecules

Biphenyl is widely used as a core framework for liquid crystals, functionalised polymers, and chiral ligands [10]. Biphenyl and its derivatives have attracted great interest due to the conformational lability associated with the low barrier of rotation around the central bond [11]. This results in changes of conformation in different phase transitions. For example, biphenyl and 4,4'-difluorobiphenyl have dihedral angles between the aromatic rings of approximately 44° in the vapour phase, whereas the molecules are planar in the solid state. The dihedral angle for the non-*ortho*-disubstituted biphenyl derivatives does not seem to be influenced by substitution in the *meta* and *para* positions. In contrast, the optimal dihedral angle varied considerably, depending on the type of atom or group in the *ortho* position of the biphenyl. The deformations of benzene caused by different substituents have been derived from high-quality X-ray data [12, 13] and it has been suggested that these substitutions are additive [12, 14]. This assumption has been tested for bromo-, chloro-, fluoro- and nitro derivatives of biphenyl and proved to be a good approximation [15, 16]. A comparison of the results obtained for 4,4'-DNBP in the gas phase and in the crystal indicate that all the geometrical parameters are very similar (within experimental error) with the exception of the dihedral angles [11].

The structure of 4,4'-DNBP, was first determined by Van Niekerk in 1943. The structure received some attention as one of the few possible examples of a centrosymmetric molecules crystallising in a non-centrosymmetric space group [17]. These doubts were first removed by Herbstein and Schoening during 1957 after their re-determination of the space group of 4,4'-DNBP which was found to crystallise in the monoclinic space group Pc and theoretical predictions based on the intensity distributions from centrosymmetric molecules in a non-centrosymmetric space group [18]. Kitaigorodskii argued [19], on the basis of the theory of close packing that the molecules should not be centrosymmetric when packed in a non-centrosymmetric space group. It was suggested that interactions between the hydrogen atoms in the *ortho* position prevent the molecule from being planar and hence from being centrosymmetric [19]. This led to a further single crystal investigation by Van Niekerk and Boonstra who showed that the orientation of 4,4'-DNBP is such that the benzene rings and nitro-groups are twisted in a helical fashion about the long axis of the molecule, hence non-planar and thus non-centrosymmetric [5].

1.1.2 Molecular Complexes of 4,4'-DNBP

An interesting characteristic of 4,4'-DNBP is its great selectivity in the formation of molecular complexes which have been obtained only with 4-substituted and 4,4'-disubstitued biphenyl molecules. Biphenyl derivatives with relatively strong electron-donating substituents such as -NH_2 or –OH groups in one or both of the *ortho* positions have failed even to generate colour on admixture with 4,4'-DNBP in solution. No evidence has been obtained of complex formation between 2,2'-DNBP and any of a large number of simple biphenyl derivatives. In the cases studied, no complex formation was observed between 4,4'-DNBP and biphenyl derivatives with electron-withdrawing groups in the *para* position. It appears therefore that electron-donating substituents favour and electron-accepting substituents inhibit complex formation [7].

The crystal structures of a number of molecular complexes formed by 4,4'-DNBP with various derivatives have been described by Rapson and Saunder [7]. The structure of C-4OHBP has been studied in some detail, and the studies of some of the other complexes demonstrated that they all possess structures of the type indicated in Figure 1 and are isostructural with C-4OHBP [7]. No X-ray data except that for the C-4OHBP are reported in this publication.

In the actual structures examined, geometrical and symmetry conditions require that the individual molecules should be tilted in varying degrees around their central C-C-sigma bonds, but the type of structure still remains essentially the same (see Figure 1) [7, 20]. The molecular phenyl packing is quite unusual. The rings of 4,4'-DNBP molecules pack in a face-centred array and form layers. The 4,4'-DNBP molecules in different layers are approximately parallel to one another and separated by a short distance of 3.7 Å [7, 20]. Thus, the planes containing the phenyl rings of the other component molecules are approximately perpendicular to those of the 4,4'-DNBP molecules.

Figure 1 Two-dimensional projection of the idealised structure for the complexes of 4,4'-DNBP

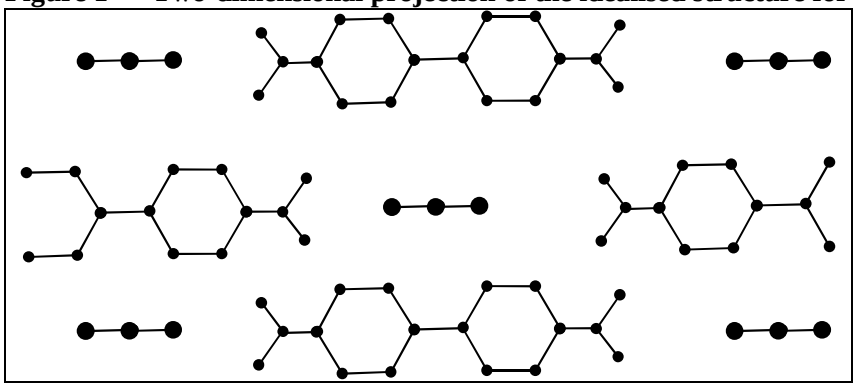

Each molecule of 4,4'-DNBP, with atoms indicated by the smaller black dots, should be seen as several molecules, one above the other, separated by a distance of approximately 3.7 Å. The larger black dots represent the atoms of the biphenyl nucleus of the other component of the complex.

In the complex C-4OHBP all the acceptor and donor molecules are approximately equally spaced in relation to one another and none of the intermolecular distances is shorter than those usually found in crystals of aromatic compounds containing nitro substituents where the bonding is attributed to Van der Waals forces. The only exception is one -OH…O- nonbonded distance of 3.0 Å. A weak hydrogen bond may thus exist but this does not fully account for complex formation as the molecular ratio of the components (4OHBP: 4,4'-DNBP) is 3:1. The closest intermolecular distance of 3.2 Å is that between the oxygen atoms of the nitro groups and the carbon atoms of the benzene rings. It is unlikely that these could provide a mechanism for complex formation particularly as the approach of the nitro groups to the phenyl ring of the 4-OHBP molecule is no closer than its approach to the phenyl ring of the 4-DNBP molecule with itself. The same almost certainly holds for the other compounds in this study for which preliminary structures have been done. In no case is there any necessity to assume closer

approach between the molecules of the components than those determined for C-4OHBP. There is sufficient space in the unit cell in each case, for the molecules to pack in a similar arrangement based on the fact that the crystal densities are as expected, and no higher than those recorded for the aromatic nitro–compounds [7, 20]. Table 2 gives the densities of some aromatic nitro-compounds and those of the complexes from the literature [7, 20].

Table 2 Densities of aromatic nitro-compounds and those of the complexes [7, 20]

Complexes	Density (g/ mL)
C-BZ	1.44
C-tmethylbz11	No data available
C-tmethylbz41	1.43
C-4OHBP	1.43
C-BP	No data available
C-4BrBP	1.52
C-44DiOHBP	1.45
4,4'-DNBP	1.45
para-dinitrobenzene	1.64
meta-dinitrobenzene	1.57

In compounds that conform to the type of structure depicted in Figure 1, the number of 4,4’-DNBP molecules that can be accommodated by each molecule of the donor component depends on the length of the molecule of this component. The tmethylbz complexes are an exception as these are two different complexes with different ratios formed from the same compounds. Rapson and Saunder calculated molecular ratios on this basis and the agreement between the observed and the calculated values are interpreted as resulting from the tilting of the various molecules. It seems evident that the exact ratios observed in these molecular compounds result of the packing rather than being controlled by bonding mechanism [7].

Abe, Matsunga and Saito [21] measured the diffuse reflectance spectrum of C-tmethylbz11 and C-tmethylbz41, which they interpreted as these complexes displaying some charge transfer. However, the polarised single-crystal absorption spectrum on C-BP shows no charge transfer [22]. It is clear that an in depth spectroscopic study of these types of complexes is required to be in a position to describe the interactions between the various components.

CHAPTER 2 Synthesis and NMR characterisation

2.1 Experimental

The compound 4,4'-DNBP was synthesised with high purity in our laboratory (Chemistry Department, Pretoria University, South Africa). The other parent compounds with electron-donating substituents were obtained from Sigma-Aldrich, except BZ of unknown origin, from the Pretoria University Chemistry Department Chemical Store. The quality of BZ was confirmed using powder diffraction, spectroscopic and thermochemical analyses.

2.1.1 Synthesis of 4,4'-DNBP

A mixture of 4-bromonitrobenzene (202 mg, 1 mmol), TDAE (0.14 ml, 0.6 mmol) and $PdCl_2(PhCN)_2$ (19 mg, 0.05 mmol) in DMF (5 ml) was refluxed under argon at 50 ºC for 4 hours. The reaction was quenched with a saturated NaCl solution and the phases were then separated. Recrystallisation from chloroform afforded 4,4'-DNBP (98.9 mg, 81%) [10]. Rf 0.17 (hexane – ethyl acetate 95:5)

2.1.2 Synthesis of Complexes

The molecular ratios used for the preparation of the various complexes were based on the ratios reported in the literature (see Table 1). The following general method was used: a considerable excess of the donor compound dissolved in acetone was added to a boiling, almost saturated solution of 4,4'-DNBP in acetone. The crystals of the molecular compounds, which separated on slow cooling, were filtered off rapidly, washed on the filter with a little acetone, and dried [7].

2.2 Nuclear Magnetic Resonance Spectroscopy

Nuclear magnetic resonance (NMR) spectroscopy is an analytical method that assists chemists identify and analyse a molecule that has magnetic nuclei by applying a magnetic field [23]. The main use of NMR in this study is in the determination and comparison of the chemical shifts of the parent compounds with those of the components in complexes, and to determine the molecular ratio of the various components in the complexes.

2.2.1 Experimental

NMR spectra were recorded on a Bruker ARX-300 spectrometer operating at 300.13 MHz for ^{1}H and 75.47 MHz for ^{13}C. All chemical shifts are reported as δ-values downfield from DMSO-d_6 (δ_H=2.49 and δ_C=39.5 for DMSO-d_6).

The spectra of parent compounds and complexes were recorded at 60ºC, due to the solubility problems of the complexes at lower temperatures. The components of the complexes were identified by comparison of the NMR spectra of the parent compounds. The molecular ratios of the components in the complexes were determined by comparison of the integrals of the respective aromatic regions for the components in the ^{1}H -spectra [Refer to Sect. 2.2.3].

2.2.2 Results

For clarity the results obtained are grouped to include those for the constituents and for the complexes in each table.

2.2.2.1 4,4'-DNBP, BZ and C-BZ

Table 3 ^{1}H chemical shifts (δ) of 4,4'-DNBP, BZ and C-BZ

4,4'-DNBP	BZ	C-BZ
8.34 (m; 4H); 8.05 (m; 4H)		8.34 (m; 4H); 8.04 (m; 4H)
	7.20 (m; 4H); 6.60 (m; 4H); 4.80 (singlet; 2H; NH_2)	7.18 (m; 4H); 6.59 (m; 4H); 4.94 (singlet; 2H; NH_2)

Table 4 **^{13}C chemical shifts (δ) of 4,4'-DNBP, BZ and C-BZ**

4,4'-DNBP	BZ	C-BZ
147.7; 128.7; 144.2; 124.2	146.5; 128.8; 125.8; 114.3	146.5; 143.9; 128.4; 125.7; 123.9; 114.2

2.2.2.2 4,4'-DNBP, tmethylbz and C-tmethylbz11

Table 5 **^{1}H chemical shifts (δ) of 4,4'-DNBP, tmethylbz and C-tmethylbz11**

4,4'-DNBP	tmethylbz	C-tmethylbz11
8.34 (m; 4H); 8.05 (m; 4H)	7.39 (m; 4H); 6.75 (m; 4H); 2.89 (singlet; 9H; NMe_2)	8.33 (m; 4H); 8.04(m; 4H) 7.38 (m; 4H); 6.72 (m, 4H);2.89 (singlet; 12H; NMe_2)

Table 6 **^{13}C chemical shifts (δ) of 4,4'-DNBP, tmethylbz and C-tmethylbz11**

4,4'-DNBP	tmethylbz	C-tmethylbz11
147.7; 128.7; 144.2; 124.2	148.9; 128.4; 125.8; 112.7	147.5; 144.0; 128.4; 125.9; 112.8

2.2.2.3 4,4'-DNBP, tmethylbz and C-tmethylbz41

Table 7 **^{1}H chemical shifts (δ) of 4,4'-DNBP, tmethylbz and C-tmethylbz41**

4,4-DNBP	tmethylbz	C-tmethylbz41
8.34 (m; 4H); 8.05 (m; 4H)	7.39 (m; 4H); 6.75 (m; 4H); 2.89 (singlet; 12H; NMe_2)	8.35 (m; 4H); 8.07 (m; 4H) 7.39 (m; 4H); 6.75 (m; 4H); 2.89 (singlet; 12H; NMe_2)

Table 8 **^{13}C chemical shifts (δ) of 4,4'-DNBP, tmethylbz and C-tmethylbz41**

4,4'-DNBP	tmethylbz	C-tmethylbz41
147.7; 128.7; 144.2; 124.2	148.9; 128.4; 125.8; 112.7	No data is available

2.2.2.4 4,4'-DNBP, 4-OHBP and C-4OHBP

Table 9 **^{1}H chemical shifts (δ) of 4,4'-DNBP, 4-OHBP and C-4OHBP**

4,4'-DNBP	4-OHBP	C-4OHBP
8.34 (m; 4H); 8.05 (m; 4H)	9.31 (singlet; H; OH); 7.20 (m; 9H);	8.32 (m; 4H); 8.04 (m; 4H) 7.50 (m; 4H)

Table 10 **^{13}C chemical shifts (δ) of 4,4'-DNBP, 4-OHBP and C-4OHBP**

4,4'-DNBP	4-OHBP	C-4OHBP
147.7; 128.7; 144.2; 124.2	156.9; 140.1; 130.9; 128.5; 127.4; 126.0; 125.7; 115.5; 56.4	147.5; 144.0; 128.6; 128.4; 127.1; 126.4; 123.9

2.2.2.5 4,4'-DNBP, BP and C-BP

Table 11 ^{1}H chemical shifts (δ) of 4,4'-DNBP, BP and C-BP

4,4'-DNBP	BP	C-BP
8.34 (m; 4H); 8.05 (m; 4H)	7.49 (m; 10H)	8.31 (m; 4H); 8.01 (m; 4H) 7.18 (m; 10H)

Table 12 ^{13}C chemical shifts (δ) of 4,4'-DNBP, BP and C-BP

4,4'-DNBP	BP	C-BP
147.7; 128.7; 144.2; 124.2	140.0; 128.5; 127.0; 126.3	157.0; 147.7; 144.1; 128.7; 128.6; 127.6; 126.2; 125.9; 124.0; 115.7

2.2.2.6 4,4'-DNBP, 4-BrBP and C-4BrBP

Table 13 ^{1}H chemical shifts (δ) of 4,4'-DNBP, 4-BrBP and C-4BrBP

4,4'-DNBP	4-BrBP	C-4OHBP
8.34 (m; 4H); 8.05 (m; 4H)	7.55 (m; 4H)	8.34 (m; 4H); 8.04 (m; 4H) 7.51 (m; 4H)

Table 14 ^{13}C chemical shifts (δ) of 4,4'-DNBP, 4-BrBP and C-4BrBP

4,4'-DNBP	4-BrBP	C-4OHBP
147.7; 128.7; 144.2; 124.2	139.1; 138.6; 131.4; 128.6; 128.4; 127.4; 126.2; 120.5; 56.3	No data available

2.2.2.7 4,4'-DNBP, 4,4'-DiOHBP and C-44DiOHBP

Table 15 ^{1}H chemical shifts (δ) of 4,4'-DNBP, 4,4'-DiOHBP and C-44DiOHBP

4,4'-DNBP	4,4'-DiOHBP	C-44DiOHBP
8.34 (m; 4H); 8.05 (m; 4H)	9.20 (singlet; 2H; OH); 7.36 (m; 4H); 6.81 (m; 4H)	8.34 (m; 4H); 8.05 (m; 4H) 7.34 (m; 4H); 6.78 (m, 4H)

Table 16 ^{13}C chemical shifts (δ) of 4,4'-DNBP, 4,4-DiOHBP and C-44DiOHBP

4,4'-DNBP	4,4-DiOHBP	C-44DiOHBP
147.7; 128.7; 144.2; 124.2	156.1; 131.2; 126.8; 115.5	156.0; 128.4; 126.7; 123.8; 115.3

2.2.3 Molecular ratio of components in the complexes

C-BZ	4,4'-DNBP: BZ	**3:1**	(lit 4:1 [7])
C-tmethylbz11....	4,4'-DNBP: tmethylbz	**1:1**	(lit 1:1 [7])
C-tmethylbz41....	4,4'-DNBP: tmethylbz	**4:1**	(lit 4:1 [7])
C-4OHBP	4,4'-DNBP: 4-OHBP	**3:1**	(lit 3:1 [7])
C-BP.....	4,4'-DNBP: BP	**4:1**	(lit 3:1 [7])
C-4BrBP.....	4,4'-DNBP: 4-BrBP	**3:1**	(lit 3.5:1 [7]
C-44DiOHBP	4,4'-DNBP: 4,4-DiOHBP	**2:1**	(lit 3:1 [7])

2.3 Discussion

Chemical shifts of parent compounds are compared with their complexes in order to allow observation of the changes in the chemical environment of the parent compounds after complex formation. Only very small changes in chemical shifts were observed. As these solutions did not maintain the colour of complexation after dissolving completely, this could be considered as supportive proof that all the interactions involved in the formation of these complexes are very weak.

The molecular ratios determined by NMR studies for C-BZ, C-BP, C-4BrBP and C-44DiOHBP are not in agreement with those reported in the literature (see 2.2.3), which are most likely incorrect. C-BZ, C-BP, C-4BrBP and C-44DiOHBP have different molecular ratios than those reported in the literature The literature ratios are most probably based on the ratio of the compounds used for the preparation of these complexes. In the present study, the crystals are isolated and dried before they are dissolved. Since the structures of the complexes were never determined the results reported in the literature are incomplete and in doubt. NMR offers a suitable method for the determination of molecular ratios, provided that the complexes are completely dissolved in the solvent. The correctness of the molecular ratios is of importance, especially for the crystallographic determination of the structure of the complexes since this will yield information of the unit cell content.

CHAPTER 3 Thermogravimetry and Differential Scanning Calorimetry

3.1 Introduction

Thermogravimetry (TG) is concerned with the change in mass of a material as a function of temperature changes. Firstly, this determines the temperature at which the material loses mass. This loss indicates decomposition or evaporation of the sample. Secondly, the temperature range at which no mass loss takes place is revealed, which indicates stability of material. These temperature ranges are physical properties of chemical compounds, and can be used for their identification in combination with other methods of analysis [24].

Differential Scanning Calorimetry (DSC) measures physical and chemical transitions. It is a more accurate method than the related technique called Differential Thermal Analysis (DTA), due to the continuous monitoring of DSC, and thereby its capacity to compensate for the imbalance of temperature which occurs in the sample and reference cells [24].

Transitions can be exothermic or endothermic. The input of energy corresponds to an endothermic effect. A typical example is the melting process, since energy is required to overcome forces that hold the sample in the solid state. Solid-solid transition, vaporisation, sublimation, desorption, decomposition and solid-solid reaction can also be described as endothermic processes [25, 26]. Conversely freezing is an exothermic process because thermal energy is released as the sample crystallises from a melt. Other exothermic processes can be seen in solid-solid transition, crystallisation, adsorption, decomposition, curing and solid-solid reactions. In the following thermograms, endothermic peaks point upward whereas the exothermic peaks point downward [25, 26].

The interpretation of thermograms is facilitated when both a TG thermogram and a DSC thermogram are obtained for the sample. The appearance of a peak on both curves indicates that the sample has undergone a weight loss. The appearance of a peak in the DSC curve but not the

TG curve discloses that the change did not involve a weight loss but must have been caused by a phase change, such as melting [24].

3.2 Experimental

TG-DSC measurements are recorded in STA 409 EP NETZCH and TA control system NETZCH with an acquisition rate of 1.5 points/ K and a heating rate of 5 K/ min in platinum crucibles open to the atmosphere. All the compounds except 4,4'-DNBP and C-4OHBP were run over the temperature range 10-410ºC. 4,4'-DNBP and C-4OHBP were run from 20-320ºC and 20-420ºC, respectively. As all the melting points of the samples in this study occur below 320ºC, the graphs were terminated at 320ºC.

3.3 Results

3.3.1 4,4'-DNBP

Figure 2 TG-DSC thermogram of 4,4'-DNBP

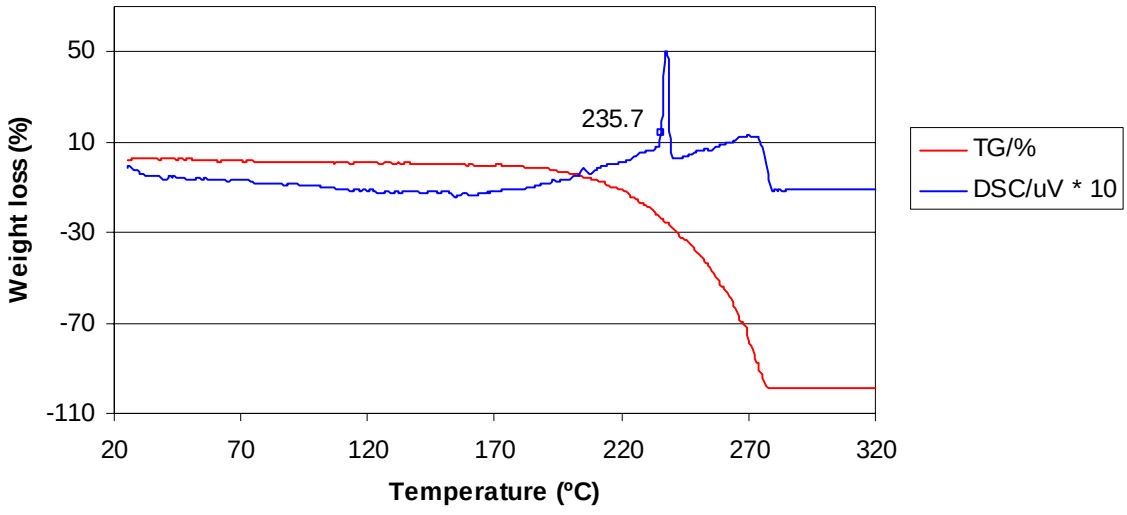

Sample weight 2.8 mg., melting point 235.7ºC (lit. 240ºC [27]). The second peak after the melting point is most likely due to evaporation.

3.3.2 BZ

Figure 3 TG-DSC thermogram of BZ

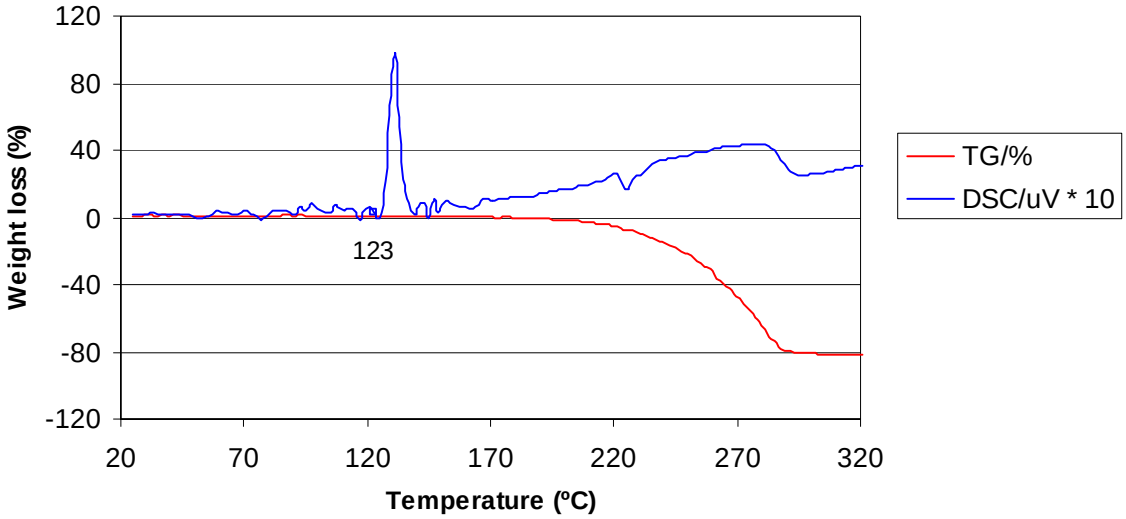

Sample weight 9.1 mg., melting point 123ºC (lit. 127ºC [28]). The other changes in the DSC thermogram can be an indication of both evaporation and decomposition of BZ since it is an extremely light-sensitive compound.

3.3.3 tmethylbz

Figure 4 TG-DSC thermogram of tmethylbz

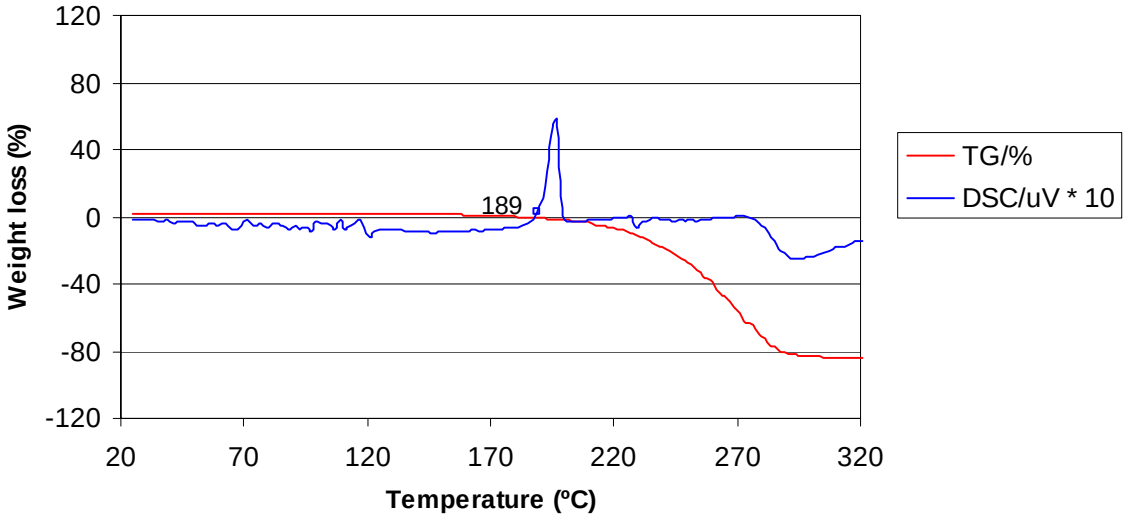

Sample weight 8.4 mg., melting point 189ºC (lit. 195ºC [29]).

3.3.4 4-OHBP

Figure 5 TG-DSC thermogram of 4-OHBP

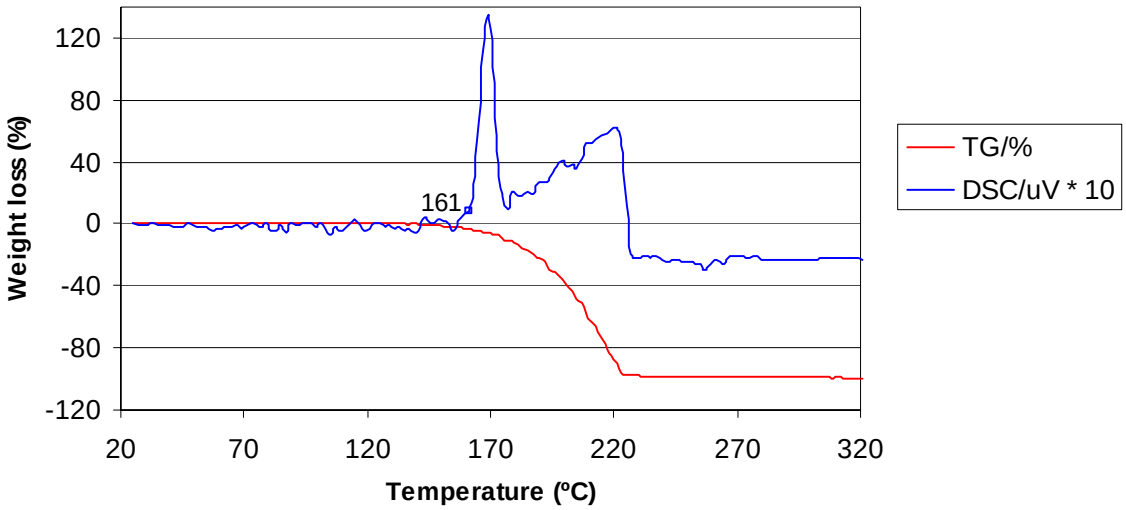

Sample weight 10.7 mg., melting point 161ºC (lit.164-165ºC [30]). The second peak after the melting point is most likely due to evaporation.

3.3.5 BP

Figure 6 TG-DSC thermogram of BP

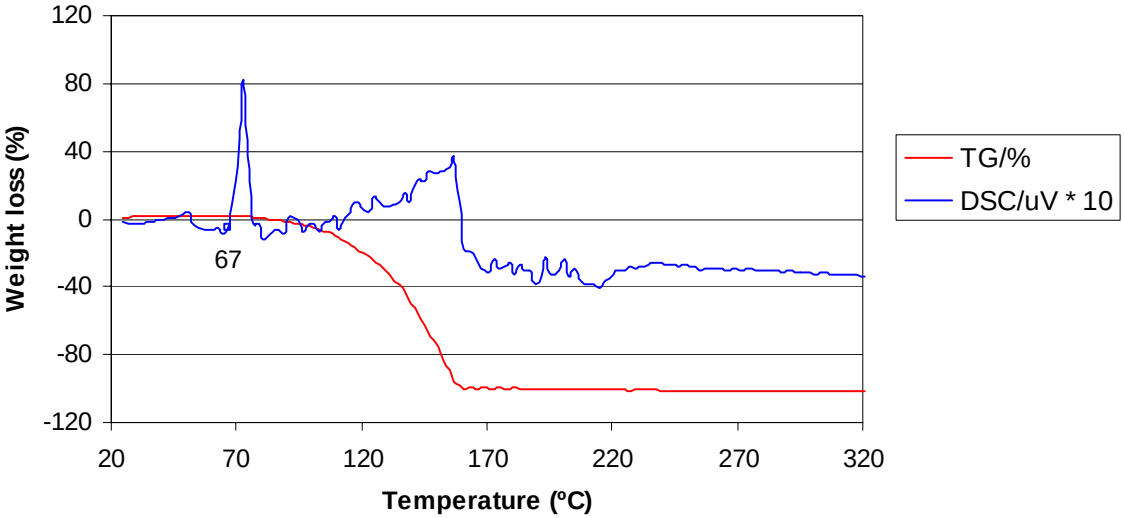

Sample weight 8.7 mg., melting point 67ºC (lit. 70ºC [28]).

3.3.6 4-BrBP

Figure 7 TG-DSC thermogram of 4-BrBP

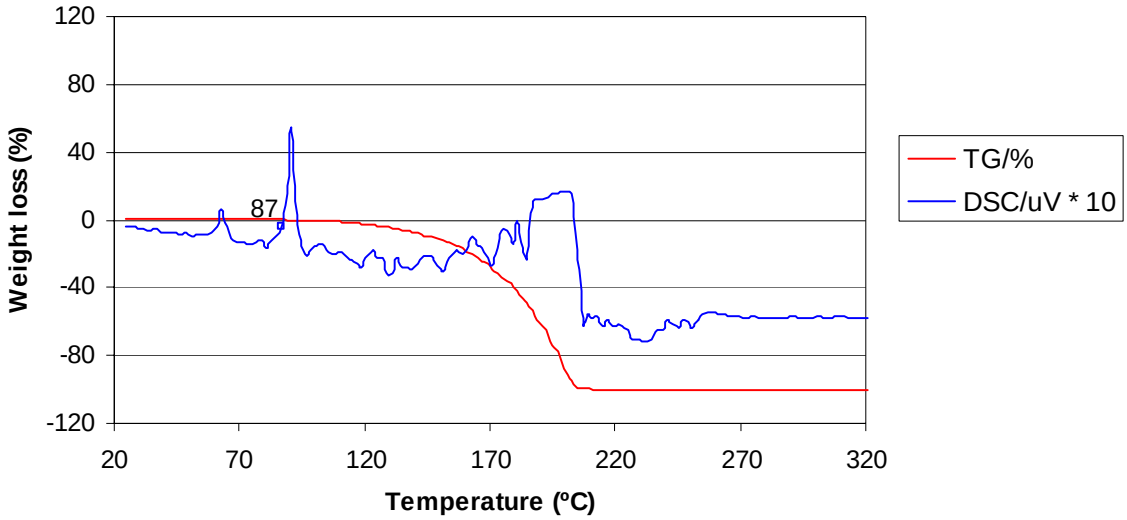

Sample weight 12.0 mg., melting point 87ºC (lit. 89-90ºC [31]).

3.3.7 4,4'-DiOHBP

Figure 8 TG-DSC thermogram of 4,4'-DiOHBP

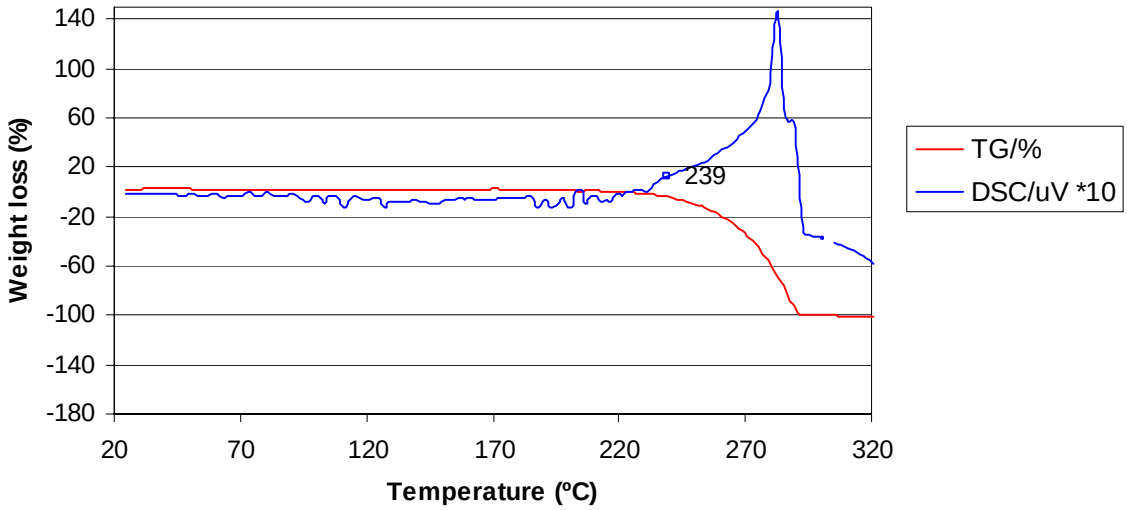

Sample weight taken is 8.7 mg., melting point is approximately 239ºC.

3.3.8 C-BZ

Figure 9 TG-DSC thermogram of C-BZ

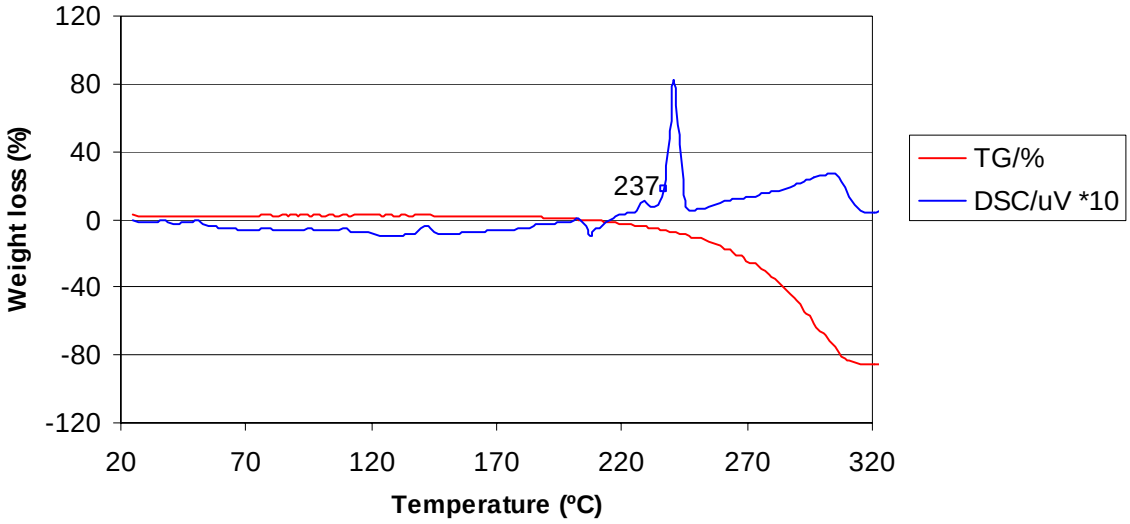

Sample weight taken is 10.5 mg., melting point is 237ºC (lit. 240ºC [7]).

3.3.9 C-tmethylbz11

Figure 10 TG-DSC thermogram of C-tmethylbz11

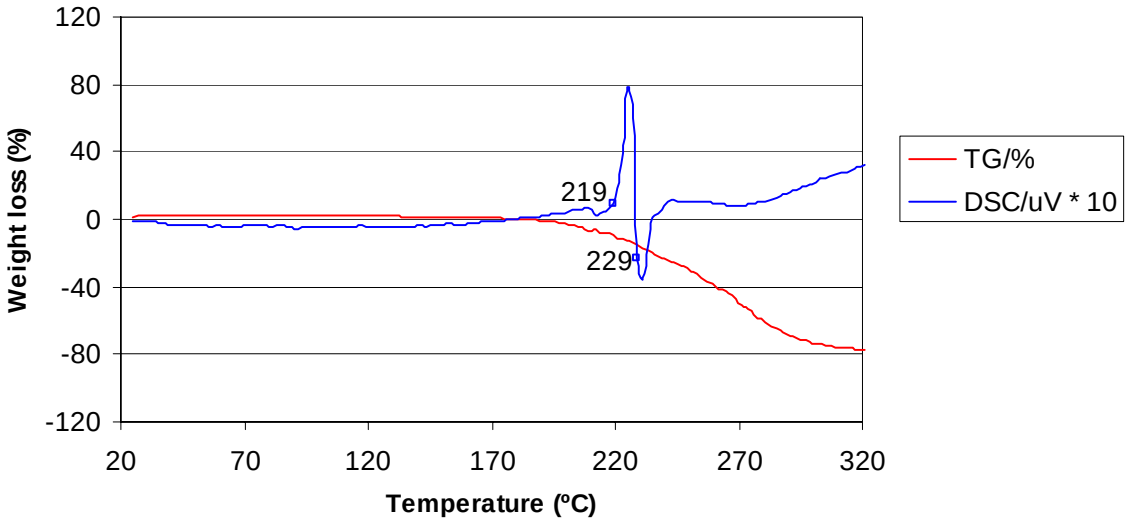

Sample weight 7.2 mg, melting point 219ºC (lit. 224ºC [7]). There is likely to be an exothermic phase relaxation or decomposition at around 229ºC. This may be due to the rearrangement of the crystalline form (different packing).

3.3.10 C-tmethylbz41

Figure 11 TG-DSC thermogram of C-tmethylbz41

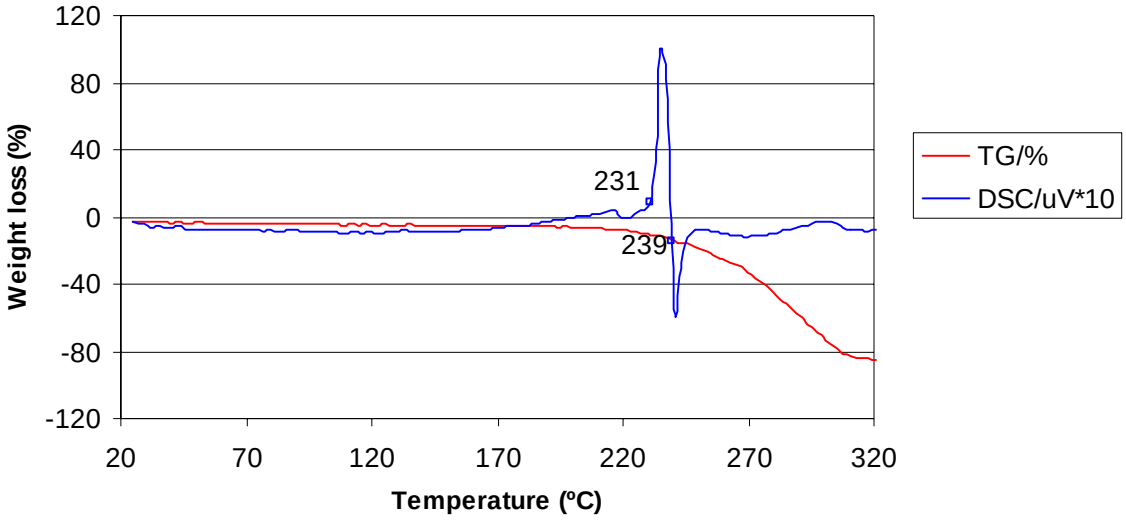

Sample weight 9.0 mg., melting point 231ºC (lit. 233ºC [7]). There is likely to be an exothermic phase relaxation or decomposition at around 239ºC. This may be due to the rearrangement of the crystalline form (different packing).

3.3.11 C-4OHBP

Figure 12 TG-DSC thermogram of C-4OHBP

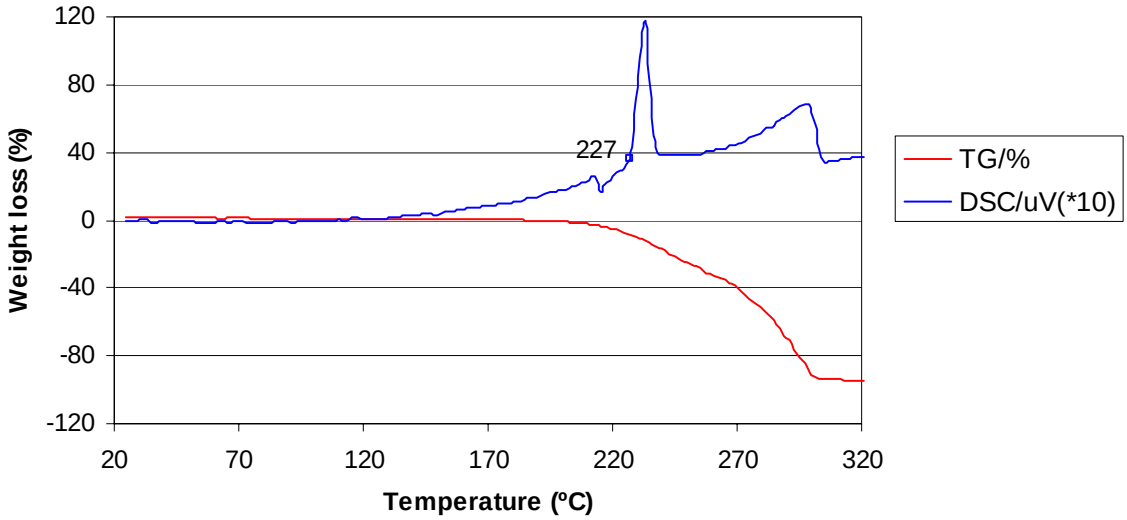

Sample weight 8.6 mg, melting point 227ºC (lit. 228-230ºC [7]).

3.3.12 C-BP

Figure 13 TG-DSC thermogram of C-BP

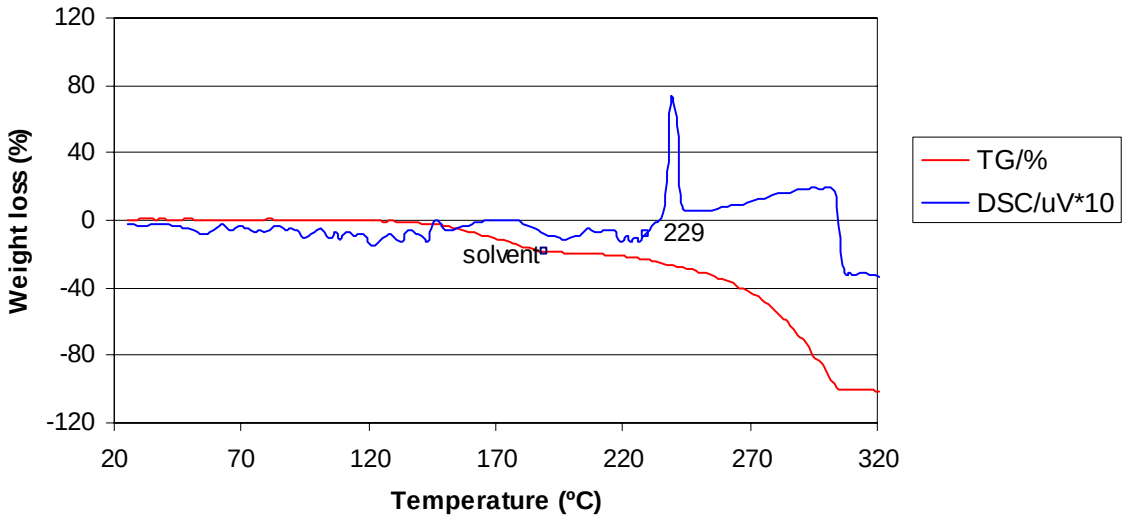

Sample weight 9.3 mg, melting point 229ºC (lit. 228-230ºC [7]).

3.3.13 C-4BrBP

Figure 14 TG-DSC thermogram of C-4BrBP

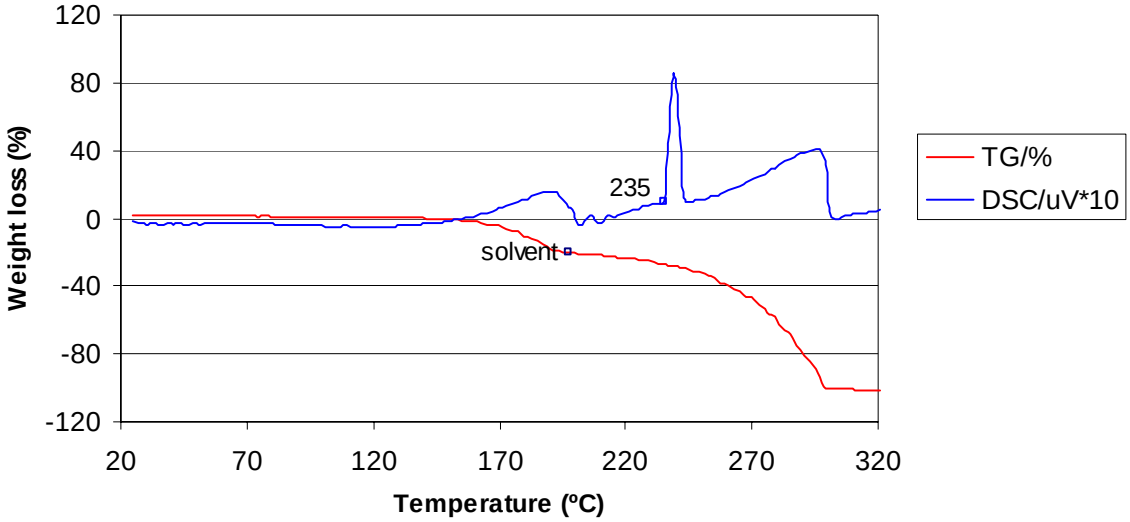

Sample weight 7.7 mg., melting point 235ºC (lit. 192-220ºC [7]).

3.3.14 C-44DiOHBP

Figure 15 TG-DSC thermogram of C-44DiOHBP

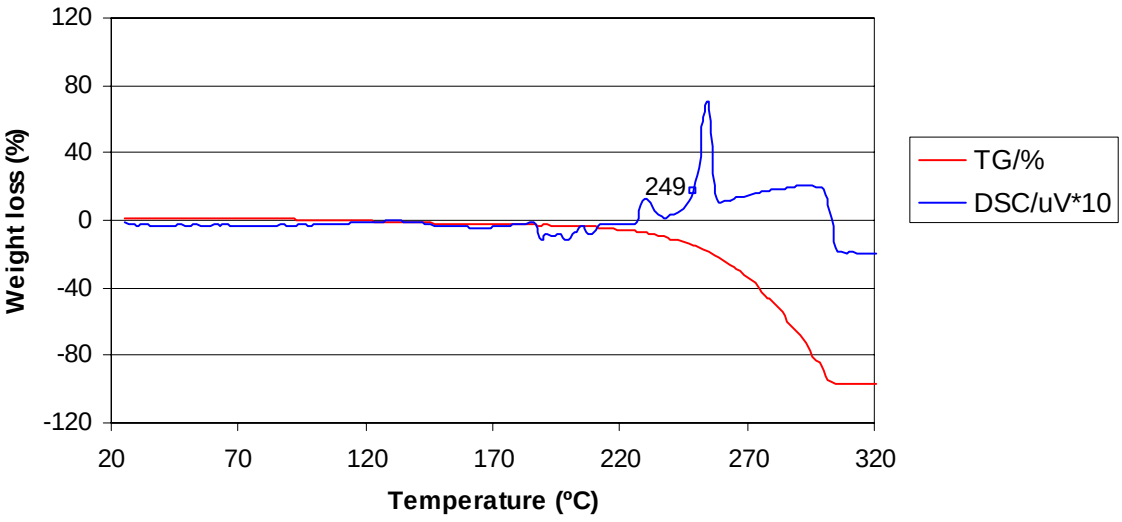

Sample weight taken is 7.7 mg., melting point is 249ºC (lit. 249-250ºC [7]).

3.4 Discussion

There are some difficulties between the melting points reported in the literature and those obtained during the experiments performed in this study. This may be due to the different reference points taken as melting points on the thermograms. This study took the first gradient of the peak as the melting point.

Naturally the different references are not the only sources of differences in TG and DSC curves. Many factors influence the form of the TG curve, both sample and instrument-related, some of which are interactive. The primary factors are heating rate and sample size, an increase in either of which tends to increase the temperature at which sample decomposition occurs, and to decrease the resolution between successive mass losses. The particle size of the sample material, the way in which it is packed, the crucible shape, and the gas flow rate can also affect the progress of the reaction [32] and the change in physical properties of a compound is attributed to its polarizability, molecular weight and molecular shape [33].

By comparison of some physical properties of these molecular complexes versus the melting point, this study hopes to determine and understand which of these factors influences the increase or decrease in the melting points of the complexes. Table 17 summarises the melting points of the parent compounds and those of the molecular complexes in this study to permit a general overview to the reader.

Table 17 Comparison of melting points between parental compounds and the components in the molecular complexes

Parent compounds	Melting points (ºC)	Molecular compounds	Melting points (ºC)
4,4’-DNBP	236		
BZ	123	C-BZ	237
tmethylbz	189	C-tmethylbz11	219
tmethylbz	189	C-tmethylbz41	231
4-OHBP	161	C-4OHBP	227
BP	67	C-BP	229
4-BrBP	87	C-4BrBP	227
4,4'-DiOHBP	239	C-44DiOHBP	249

In Figure 16, the melting points of the complexes are plotted with respect to their intensity or strength of colour. The dots in the figure are the actual colours observed for each complex. C-4BrBP has the lightest colour and C-tmethylbz11 the darkest colour (see Table 1 for the details of colours). There seems to be no correlation between colour and the increase or decrease of melting point.

Figure 16 Comparison of melting points of the complexes with respect to the strength of their colour

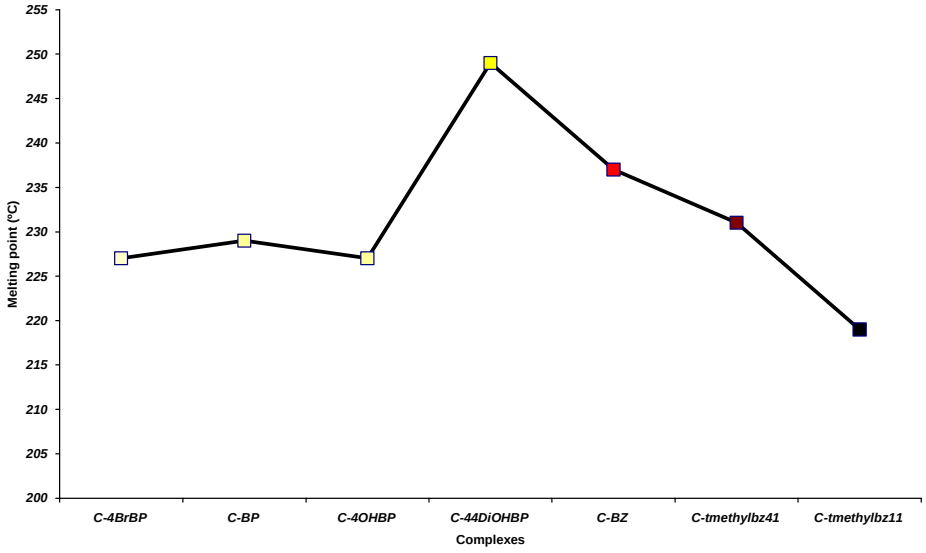

In Figure 17, the melting points of complexes are compared with respect to the molecular ratios of both 4,4'-DNBP and the donor components in the complexes. A change in 4,4'-DNBP ratio to the donor component in a complex seems, in general, to have no effect in melting point.

Figure 17 Comparison of melting points of the complexes with respect to the relative ratio of 4,4'-DNBP to the donor component in the complex

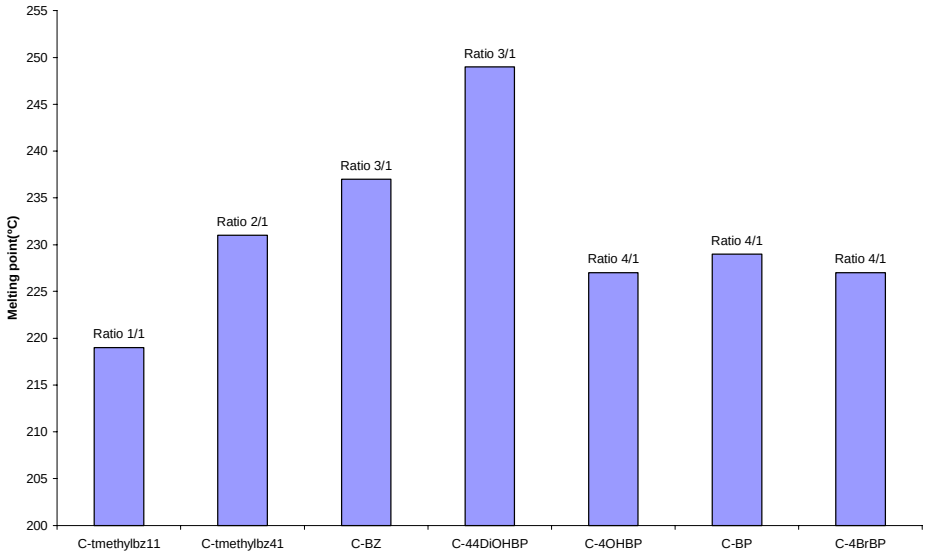

The change in physical properties of a compound may be attributed to its polarizability as well. As the *polarizability* is the ease with which a dipole can be induced in an atom or molecule, it increases with increased numbers of electrons in a species (see CHAPTER 1 for the definition of polarizability). The number of electrons is related in general to the molecular weight. Because dispersion forces become stronger as polarizability increases, in general melting points and boiling points increase with increasing molecular weight [33].

Therefore, Figure 18 compares the role of molecular weight of complexes with changes in melting points. If only polarizability plays a role, a direct relation is expected between molecular weights and melting points. However, C-BZ and C-44DiOHBP do not fit into this pattern. Their melting points are higher than the other complexes with larger molecular weight. This may be an indication of a stronger interaction in C-BZ and C-44'DiOHBP. C-44DiOHBP (with two OH groups attached to one biphenyl component and two nitro groups in the other component) might have additional influence than other components to 4,4'-DNBP, due to its capacity to form hydrogen bonds. The other molecules that may participate in hydrogen bonding are C-BZ (with two NH_2-groups in one component and nitro-groups in the other) and C-4OHBP (with one OH-group in one component and nitro-groups in the other). However, it is noticeable that the melting point of C-4OHBP does not display the relatively high melting point like C-44DiOHBP and C-

BZ. Thus, it seems to be a requirement to have both para positions of BP substituted with functional groups that may form hydrogen bonds, before these compounds take part in any significant hydrogen bonding. The other complexes, however, have closely related melting points and their melting points seem to increase with increasing molecular weight.

Figure 18 Comparison of melting points with respect to increase in molecular weights of complexes

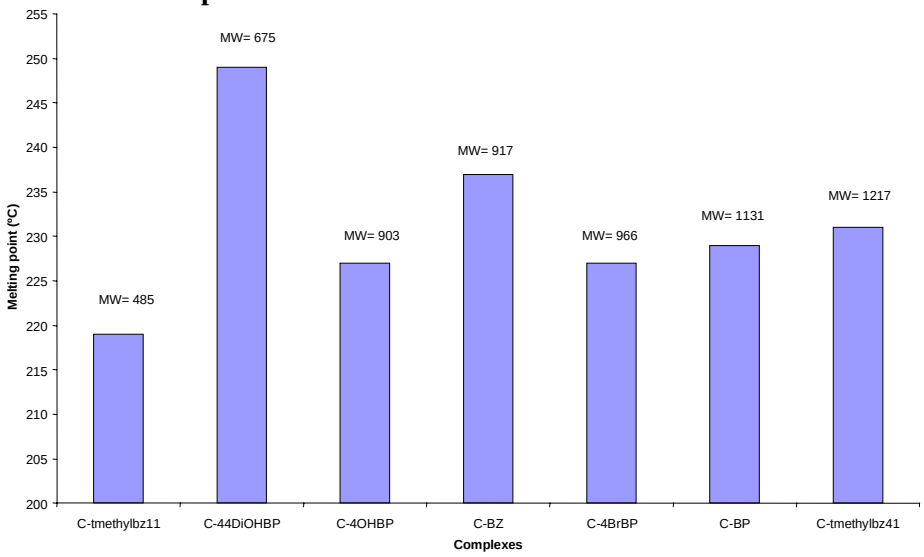

Because only the electron donor substituted *para* biphenyl compounds are able to form complexes with 4,4'-DNBP, substituents of biphenyls in the present study are reported in Figure 19 in decreasing order of their capability to donate electrons to biphenyl. Bromine is an exception in these series since it is a relatively weakly electron-withdrawing substituent: NMe_2>NH_2>OH>H>Br. However, there is no apparent relation between the capacity to donate electrons and melting points.

Figure 19 Comparison of melting points of the complexes in respect to the number and nature of substituents of biphenyls which are given in decreasing order of their capability to donate electrons

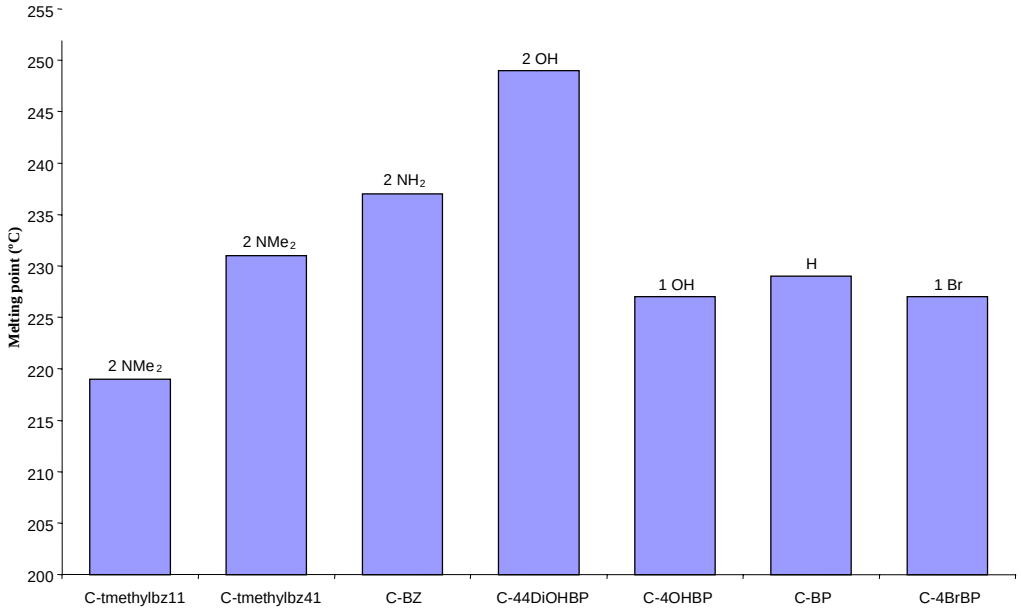

In Figure 20, the melting points of the parent compounds are compared with the melting points of the complexes. The melting points of the complexes show significant similarities with those observed for 4,4'-DNBP, and the presence of a single melting point indicates that the components in the complexes do not melt independently. This shows that the components are energetically more stable in the complexes than in parent compounds, as suggested previously by Burton and Richards in their previous infrared and Raman studies [40].

Figure 20 Comparison of the melting points of pure compounds with those of their complexes

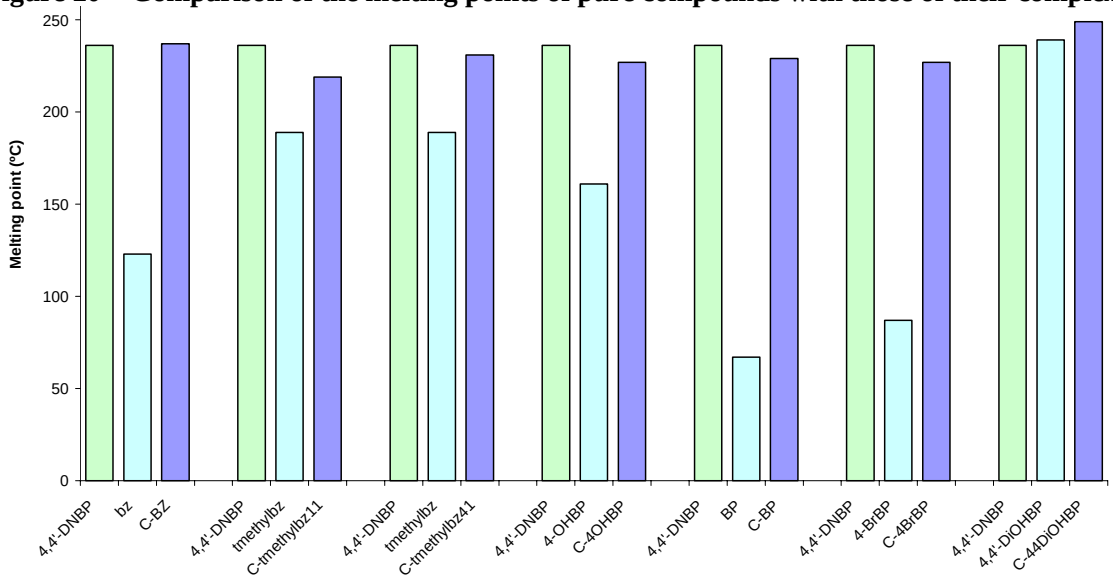

Although the comparison of melting points with respect to increase in molecular weight of complexes in Figure 18 gives an indication of the presence of hydrogen bonds in C-BZ and C-44DiOHBP, one must be careful before drawing conclusions, since there are insufficient parameters on the graphs.

CHAPTER 4 Ultraviolet-Visible Spectroscopy

4.1 Introduction

Absorption of ultraviolet and visible radiation in organic molecules is restricted to certain functional groups (chromophores) that contain valence electrons of low excitation energy. The absorption occurs when the electrons of these chromophores are excited from lower energy molecular orbitals to higher levels. UV-VIS spectrometers can rapidly scan the electronic region of the spectrum and provide evidence of the existence of characteristic chromophores. The major limitation imposed is that the compound to be detected must have a characteristic UV-VIS absorbance in the range of 220-770 nm. Absorption of energy in this region is associated with promotion of electrons to higher energy states. In organic molecules absorption of energy in this region usually requires the presence of functional groups (containing nitrogen, oxygen, sulphur and halogen atoms) or multiple bonds, especially two or more such bonds in conjugation. Saturated molecules do not absorb significantly in this region. The amount of an intermediate which can be detected depends on how strongly it absorbs relative to other components of the reaction systems. In favourable cases, concentrations as low as 10^{-6}M can be detected [34].

The spectra of π-molecular complexes are, to a good approximation presented by the sum of the spectra of the individual components. An additional absorption band which is assigned to the charge transfer (CT) band by some authors (see CHAPTER 1 for details) occurs in the near-UV, visible or near-IR region between about 5000 and 30000 cm^{-1}. The position of charge transfer bands does not affect the IR spectrum between 4000 and 700 cm^{-1} [3]. The nature of the ground state, whether ionic or non-ionic, can be determined by overall comparison of the spectrum of the molecular compound with spectra of the individual components which ionising and neutral conditions [3]. In the absence of any major interactions it can be concluded to be most likely '*dipole-dipole interaction*' [3].

Dipole-dipole interaction is an intermolecular interaction between molecules having permanent electric dipoles. This is a type of Van der Waals interaction [35].

However, some authors suggest that the major contribution to the π–π interactions come from the electrostatic and Van der Waals interactions (see CHAPTER 1) [9]. π–π Interactions rarely cause a distortion of the UV-visible spectra of the two chromophores, so the two interacting π-systems do not distort each others molecular orbitals [9]. It should be possible to explain the colour of the complexes on the basis of the ground-state wave functions of the two π-systems [9].

An increase in double bond character through conjugation requires less energy for the electronic transition and therefore a maximum absorption band appears at a longer wavelength. The presence of a sufficient number of conjugated double bonds in a compound will promote the absorption of visible light [36]. This usually occurs with longer π-orbital chains overlapping [36]. For overlap to occur, the π-system should be planar.

Empirical rules based on observations have been developed over the years relating the wavelengths of the UV absorption maxima to the structures of a molecule [24]. There are essentially four molecular systems, namely dienes, monosubstitued benzene rings, disubstituted benzene rings, and conjugated carbonyl systems. The method of calculation is to take a parent system (in the present study the biphenyl molecule) and assign an absorption maximum. The parent system is then modified by the presence of other systems within the molecule. From these modifications, the absorption maximum can be calculated [24].

4.2 Experimental

The spectra of all the compounds were obtained on a Perkin Elmer 25 in the region 200 and 700 nm at RT. Compounds were studied in both the solid state (2 mg sample/200 mg KBr) and in solution using acetonitrile as solvent. The solid state experiments did not produce any noticeable absorption, most likely due to the low quality of pellets produced.

4.3 Results

4.3.1 Solution spectra

Results from the solution spectra are tabulated in Table 18.

Table 18 Comparison of parent compounds with the components in the complexes

Parent compounds	λmax (nm)	Molecular compounds	λmax (nm)
4,4'-DNBP	308		
BZ	288	C-BZ	303
tmethylbz	310	C-tmethylbz11	309
tmethylbz	310	C-tmethylbz41	308
4-OHBP	261	C-4OHBP	308
BP	244	C-BP	308
4-BrBP	255	C-4BrBP	308
4,4'-DiOHBP	263	C-44DiOHBP	307

4.4 Discussion

None of the spectra of the complexes showed an additional band in the visible region of the spectra and it must therefore be concluded that no charge transfer occurs.

As the solutions of the complexes were dilute, the complexes did not exhibit their colour. Furthermore, C-tmethylbz11, C-tmethylbz41, C-4OHBP, C-BP, C-4BrBP and C-44DiOHBP have absorption maxima similar to the absorption maximum of 4,4'-DNBP. It may be possible that the complexes are dissociated into their pure compounds in solution. In this case the donor components are not visible because of their low contributions to the complexes. UV, being a concentration-sensitive method, failed to detect the components with low contribution in the complex. The C-tmethylbz11 was the only complex where the donor component (tmethylbz) is equimolar with 4,4'-DNBP and as such it was expected to observe two absorption maxima: one belonging to tmethylbz and one to 4,4'-DNBP. However the absorption maxima of both tmethylbz and 4,4'-DNBP compounds are coincident.

Only C-BZ shows a significant 5 nm difference from the original 4,4'-DNBP absorption which may be seen as an interaction: hydrogen bonding between the NO_2 and NH_2 functional groups is possible. The hydrogen bonding will necessitate the partial shift of more electrons to the oxygen atoms in the nitro groups thereby reducing the double bond character of the 4,4'-DNBP, and as a result the absorption maxima of the 4,4'-DNBP component of the C-BZ will appear at a shorter wavelength.

In the solution UV study it was anticipated to deduce the structural changes in the components of the complexes, by relating the wavelengths of the UV absorption maxima of the parent compounds and those of the complexes. But, the potential dissociation of complexes into their separate components put the reliability of the UV study in solution for molecular complexes at stake, making the solid state UV study a necessity. However, the liquid phase UV study gives sufficient proof that the interactions involved in these complexes are weak.

CHAPTER 5 Infrared and Raman Spectroscopy

5.1 Introduction

Raman and infrared spectroscopy measure the energy difference between vibrational energy levels in molecules. The basic principle of the two techniques differs and this results in different vibrations being active in Raman and infrared spectra.

Interaction of the infrared radiation with a vibrating molecule is only possible if the specific vibration alters the molecular dipole moment, whereas for a vibrational mode to be Raman-active the molecular polarizability must change. If a molecule has a centre of symmetry Raman-active vibrations are infrared inactive and vice versa. If there is no centre of symmetry then some (but not necessarily all) vibrations may be both Raman and infrared-active. This is known as the rule of mutual exclusion [37]. Caution is necessary in applying this rule because other factors may play a role. For instance, a vibration may be Raman-active but too weak to be observed. However, if some vibrations are observed to give coincidental Raman and infrared absorptions it is certain that the molecule has no centre of symmetry [37].

The position of a given stretch vibration in Raman and infrared spectra can be related mainly to two factors, namely: the masses of the atoms involved (lighter atoms vibrate at higher frequencies than heavier ones) and the relative strength of the bond. Triple bonds are stronger (and vibrate at higher frequencies) than double bonds and double bonds are stronger (and vibrate at higher frequencies) than single bonds. The order of bond strength can be summarised as $sp > sp^2 > sp^3$ [38].

Furthermore, the position of a vibrational band is dependent on the environment of a molecule. Molecular substituents, molecular geometry and hydrogen bonding affect the vibrational force constant which dictates the vibrational energy [38].

The aromatic symmetric stretch vibration, which is a strong band in Raman spectra reflects any change in the electron density of the benzene ring. For this reason, the parent compounds and the complexes in this study are compared using their Raman aromatic stretch bands in order to confirm any interaction in the complexes.

Infrared and Raman spectroscopy are therefore useful methods to study intermolecular interactions and can give useful information about the geometry of crystalline compounds with weak intermolecular interactions as both methods are sensitive to changes in bond lengths and symmetry of molecules.

5.1.1 Interpretation of spectra of BP compounds

The complexes and the parent compounds in this study were not thoroughly examined in the past as the spectra proved to be rather complicated. It has been found that the vibrational assignment of even the simplest molecule, biphenyl, had ambiguous assignments, most of which are based on their similarity to benzene [39]. The approach to these assignments was that biphenyl is considered a monosubstituted benzene whose substituent is a phenyl group. Indeed this gave a good similarity to biphenyl experimental bands, except for some splitting in its vibrational levels. The amount of splitting and the eventual frequency shifts depend on the strength of the C-C bond on the possible steric interactions and on the extent of kinetic coupling between the two rings [39]. Such factors help to interpret the spectra between the different biphenyl derivatives spectra.

5.1.2 Previous Infrared and Raman studies on the complexes in this study

Burton and Richards used infrared spectroscopy to study C-4OHBP and C-BP and their separate components in the solid state and in solution [40]. In this study no formal assignments of the vibrational bands were made and the spectra were analysed purely with respect to the vibrational coordinates and intensities. It was found that in the solid state, C-BP has an absorption spectrum corresponding to a simple addition of the spectra of its components, except in the region 750-850 cm^{-1}. These bands are due to the out-of-plane vibrations of the C-H bands of the benzene rings and similar small shifts in these absorption bands were observed in the solid state spectrum of C-

4OHBP. A variation in the intensity of bands in the region of the C-H ring stretch vibrations was also observed.

The same authors studied C-4OHBP and C-BP in solution [40]. The results showed that the addition of 4,4'-DNBP to a solution of 4-OHBP does not decrease the free 4-OHBP concentration as would be expected if the complex existed in solution. Although the estimation of the 4-OHBP can only be considered to be very approximate in view of other bands, the results indicate that complex formation in this solution occurs only to a very small extent, if at all [40]. In C-4OHBP and C-BP, it seems that the interaction between the polar and polarisable components is very small, if not absent. The absence of the C-4OHBP in solution, as deduced from the intensity measurements, also implies that the intermolecular attraction must be weak and is easily dominated by the solvent interactions [40]. It was proposed that the oxygen atoms of the nitro groups of 4,4'-DNBP carry fractional negative charges and if these groups approach relatively close to one another, this would cause repulsion between these nitro-groups. But when 4,4'-DNBP encounters the other components, the repulsion decreases and therefore it is able to do so in the preferred layer-type lattice, using the other components to separate or insulate the polar nitro-groups from one another [40].

In a subsequent investigation by Bolton and Prasad, both infrared and Raman spectroscopy were used to study C-4OHBP, C-BP and C-4BrBP [1]. The internal vibrations of the complexes and of the components as well as the phonon spectra were recorded at 18K, 125 K and RT. The authors deduced from both phonon and intramolecular vibrational studies that these complexes form in fixed molecular ratio, are governed by geometrical factors, and are stabilised primarily by Van der Waals interaction, although other kinds of interactions may provide additional stabilisation. In C-BP, the 4,4'-DNBP and BP molecules are centrosymmetric and remain so in the temperature range from 18 to 298K. In the complexes C-4OHBP, C-BP and C-4BrBP, crystal splitting is observed on the 410 cm^{-1} vibration of 4,4'-DNBP. This splitting was attributed to the presence of more than one 4,4'-DNBP molecule in the complex unit [1]. It is found that the vibrational frequencies of C-4OHBP, C-BP and C-BrBP are within 5 cm^{-1} of the vibrational frequencies observed in their parent compounds. According to the authors, these small shifts are well within the range of crystalline shifts ascribed to the differences in the crystal structure of the parent compounds and that of the complex. Consequently, they inferred that the complexes are formed

mainly on the basis of favorable packing and are stabilised primarily by Van der Waals interactions. They found no evidence of hydrogen bonding in these complexes [1].

5.2 Experimental

Raman spectra were recorded at room temperature with a Dilor XY Raman spectrometer, using the λ=514.5 nm laser line of a Coherent Innova 90 Ar^+-laser as excitation line. The spectra were recorded in a backscattering configuration with the Olympus microscope attached to the instrument, using a 50 X objective and a low laser power of 0.5 mW at the sample. This was necessary as the coloured samples had very high background fluorescence caused by the laser line, and also decomposed during the recordings due to laser heating. The measurements were obtained in the 400-1800 cm^{-1} region. A high fluorescence background between 2700-3000 cm^{-1} prevented the accumulation of spectra in this region.

For the solid state, mid- and far-infrared transmission spectra were recorded with a Bruker 113v Fourier transform infrared (FTIR) spectrometer. The resolution was 2 cm^{-1} and 32 scans were signal-averaged in each interferogram. The samples were pressed into KBr pellets (2 mg sample/ 100 mg KBr) and into polyethylene pellets (2 mg sample/ 20 mg polyethylene), for the mid- and far-infrared measurements, respectively. However, the results for the far-infrared region were of insufficient quality to allow correlation studies.

An attempt was also made to investigate the compounds in solution, but no spectra have been obtained.

5.3 Results

The vibrational assignments of the parent compounds and complexes in this study (except BP and BZ) were not available from the literature (see 5.1.1 for the detailed information about the previous studies on the BP molecules). The values obtained for BP [41, 42]. and BZ [43] in this study are compared with literature values and a good agreement is obtained, verifying the purity

of these samples used. All the ring vibrational assignments of the parent compounds are based on the BP and BZ structures and the assignments of all the parent compounds as well as their complexes are presented at the end of the chapter. The bands corresponding to the nitro groups in 4,4'-DNBP were assigned according to the general rules for NO_2 aromatic compounds [44].

5.3.1 BP

Both the geometry of biphenyl in solid phase and in solution was investigated. The biphenyl molecule in the solid phase appears to be planar within the limits of error [7, 45, 46]. However, the biphenyl appears to be non-planar (40º dihedral angle between the aromatic rings) in solution [47]. The present study includes biphenyl both in solid phase and in solution since the molecular complex with 4,4'-DNBP was formed in a solution.

The vibrational spectrum of biphenyl in KBr from this study is compared to the monosubstituted benzene model from the literature [41, 42]. The result is shown in Table 19.

Table 19 The vibrational wavenumber values of BP are given in cm^{-1}. Raman values are shown in brackets.

Assignment	Monosubstituted benzene [41, 42] (cm^{-1})	BP in KBr for this study (cm^{-1})
ν_{ring}	1600	1598 m (1606w and 1588w)
ν_{ring}	1568	1569 m
ν_{ring}	1483	1480 s
ν_{ring}	1460	
ν_{ring}	1431	1429 s

s = strong; m = medium; ν_{ring} = stretch vibration of the ring

5.3.2 BZ

Table 20 Comparison of the spectrum of BZ in this study with that from the literature. Vibrational wavenumbers are given in cm^{-1}. Raman values are shown in brackets.

Assignment	BZ from literature [43]		BZ from this study	
ν_{asym} (NH_2)	3431 s	(3436w)	3431m	
	3394 s	(3398w)	3394m	
ν_{sym} (NH_2)	3354 s	(3356 m)		
	3321 s	(3322 vs)	3321 m	
2δ (NH_2)	3204 s		3202 w	
ν_{ring} (CH)	3061 w			
ν_{ring} (CH)	3046 w			
ν_{ring} (CH)	3029 w		3029 w	
ν_{ring} (CH)	3007 w			
δ (NH_2)	1628 vs	(1629 s)	1627 s	
ν_{ring}	1604 vs	(1608 vs)	1605 s	(1607 vs)
ν_{ring}	1499 vs		1499 s	
			1495 s	
ν_{ring}	1412 w		1413 m	
ν_{ring}	1327 vw			
δ (CH)	1301 w			
		(1281 m)		(1281 m)
ν (CN)+ν_{ring}	1270 sh	(1266 m)		
	1266 sh			
ν CN) [48]	1262 s		1262 s	
δ (CH)	1176 s		1175 m	
δ (CH)	1140 m		1139 w	
Ring breath		(851 m)		(851 m)
Ring breath	848 m		848 m	
	815 vs		816 s	
γ_{ring}	747 m	(704 w)	749 w	

s = strong; m = medium; w = weak; v = very; br = broad; sh = shoulder; ν = stretch vibration; ν_{asym} = asymmetric stretch; ν_{sym} = symmetric stretch; δ = deformation; γ = rocking

5.3.3 The Raman bands of the aromatic stretch vibration of the pure components

Figure 21 Aromatic C=C stretch vibration of parent compounds in the Raman spectra

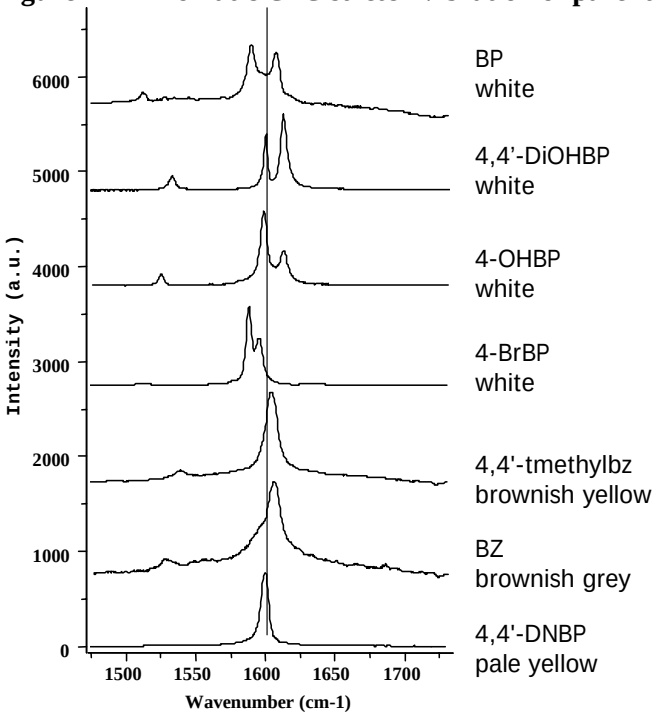

In Figure 21, the Raman spectra of the parent compounds in this study are presented in the region of the C=C aromatic stretch vibration. In the BP spectrum, two peaks (at 1589 and 1607 cm^{-1}) are observed in this region, due to vibrational coupling between the vibrations of the two rings, resulting in an in-phase and out-of-phase vibration (see Table 19 for the infrared and Raman assignments of BP in this region).

For 4-BrBP, 4-OHBP and 4,4'-DiOHBP two bands are also observed in this region. From their crystallographic studies (see *6.2.2* for the information about their central dihedral angles), it has been established that only BP, 4-OHBP and 4,4'-DiOHBP are nearly planar. For the centrosymmetric and planar 4,4'-DiOHBP compound, the band is split, similar to BP, likely due to coupling. However, the 4-OHBP and 4-BrBP are not centrosymetric, even though 4-OHBP is planar. The presence of two bands for 4-OHBP and 4-BrBP may be a result of the single substituent on the one ring, which influences the strength of the aromatic C-C bond and shifts the band relative to the ring without the hydroxy group. The shift of the bands to higher wavenumbers for the hydroxy groups (in contrast to the shift to lower wavenumbers for the

bromo-compound) may be due to the difference in electronegativity between the OH and Br substituent.

In Table 21, a correlation between the shape of the Raman aromatic C=C stretch vibration of parent compounds at 1600 cm^{-1} with the symmetry of the parent compounds was attempted. Although 4,4'-DNBP, 4-BrBP and tmethylbz are non-planar and non-centrosymmetric, the shape of the Raman aromatic C=C stretch vibration of 4,4'-DNBP and tmethylbz differ from that of 4-BrBP. In addition to this discrepancy and the fact that no data are available on the crystal structure of the BZ molecule, there are not sufficient parameters in the Table 21 to make such a correlation possible.

Table 21 Shape of the peaks at around 1600 cm^{-1} and their correlation with regard to the planarity of the parent compounds

Parent compounds	Symmetry	Shape of the peak at around 1600 cm^{-1}
4,4'-DNBP	non-planar (non-centrosymmetric)	one peak
BZ	*no data available*	one peak
tmethylbz	non-planar (non-centrosymmetric)	one peak
4-OHBP	planar (non-centrosymmetric)	two peaks
BP	planar (centrosymmetric)	two peaks
4-BrBP	non-planar (non-centrosymmetric)	two peaks
4,4'-DiOHBP	planar (centrosymmetric)	two peaks

As the aromatic stretch Raman bands of *ortho*- and *para*- dinitrobenzene are similar compounds to those of 4,4'-DNBP, their Raman bands in this region are compared to the peaks of 4,4'-DNBP. For the value of both *ortho*- and *para*-dinitrobenzene absorption occurs at 1590 cm^{-1} [49], which is similar to 1588 cm^{-1} observed for nitrobenzene. This is in accordance with the effects of the electron-withdrawing nitro group attached to the ring, which causes the bonds to be electron deficient and consequently longer, resulting in a Raman shift to lower wavenumbers from benzene at 1608 cm^{-1}. In contrast, the same band in 4,4'-DNBP occurs at 1602 cm^{-1}. A shift of the aromatic C=C bond to higher wavenumbers implies an increase in the bond order of the aromatic ring.

5.3.4 The changes of the Raman aromatic stretch vibration in complex formation

Figure 22 Raman spectra of complexes together with their parent compounds

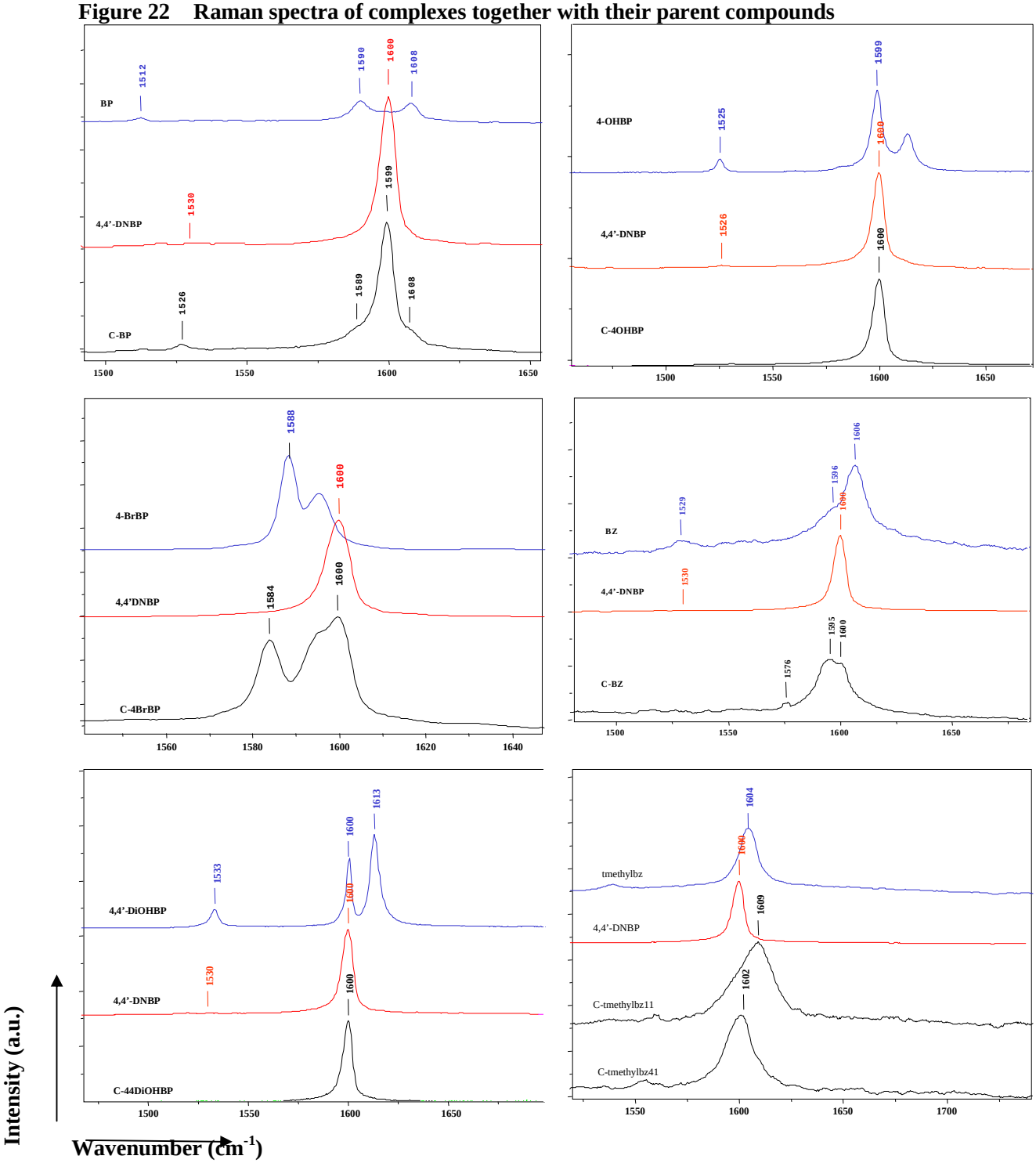

At the first glance, the peaks in all the spectra of the complexes seem to be a simple addition of the spectra of their parent compounds. However, there are some small shifts, indicating some interactions between the components in the complexes. This would make the bonds on the rings of these components either stronger or weaker. Except in the case of C-BZ, C-4-OHBP and C-44DiOHBP, the spectra of parent compounds are shifted within 5 cm^{-1} in the spectra of parent component of the molecular complex of 4,4'-DNBP. For instance, the band at 1588 cm^{-1} assigned to 4-BrBP from the parent compound has shifted to lower wavenumbers at 1584 cm^{-1} in the spectrum of the C-4BrBP. The C=C stretch vibration of 4,4'-DNBP and tmethylbz is respectively at 1604 $cm^{-1}$and 1600 cm^{-1}, although in their complexes broader bands at 1609 cm^{-1} for C-tmethylbz11 and 1602 cm-1 for C-tmethylbz41 are observed. In the spectrum of C-BP, there is a combination of the spectra of its two individual components, where there is hardly any interaction.

The spectra of C-4-OHBP and C-44DiOHBP showed unusual peaks. Although their donor components, 4-OHBP and 4,4'-DiOHBP, have two peaks, C-4OHBP and C-44DiOHBP have only one peak at 1600cm^{-1}, whose position is the same as that of 4,4'-DNBP and one of the two peaks that the 4-OHBP and 4,4'-DiOHBP components have. It is possible that the missing peaks of 4-OHBP and 4,4'-DiOHBP shifted to higher wavenumbers in the spectrum of C-4OHBP and C-44DiOHBP, indicating that the absorption of benzene rings of both 4-OHBP and 4,4'-DiOHBP in C-4OHBP and C-44DiOHBP are becoming stronger.

The spectrum of BZ compound showed a significant shift in the spectrum of C-BZ. The C=C band of the BZ compound appeared at 1606 cm^{-1} and at 1596 cm^{-1}, respectively whereas C-BZ shows a broad peak between 1600 cm^{-1} and 1595 cm^{-1}. The peak at 1600 cm^{-1} of C-BZ may represent the peak of 4,4'-DNBP, whose parent compound is in the similar position. The disappearance of the C=C band of the BZ compound at 1606 cm^{-1} may be a result of a weak interaction. This can also be an indication of hydrogen bonding between NO_2 and NH_2 substituents deduced from the UV-VIS results.

5.3.5 Comparison of the IR bands of the aromatic ring C-H stretch vibrations of the parent compounds and their complexes with 4,4'-DNBP

In Figure 23, the spectra of the parent compounds and the components of C-tmethylbz11 and C-tmethylbz41 are shown in the region 2700-3300 cm^{-1}, to illustrate the C-H symmetric and asymmetric stretch vibrations of the methyl groups of NMe_2 on the rings. The infrared spectra of the complexes and the parent compounds of C-BZ, C-4OHBP, C-BP, C-4BrBP and C-44DiOHBP, on the other hand are shown in the region 3000 – 3600 cm^{-1}. The vibrations corresponding to these regions are the C-H stretch vibrations of the aromatic rings, O-H stretch vibrations of hydroxy groups and N-H stretch vibrations.

The broad peaks at around 3400 cm^{-1} assigned to OH groups that appear in the spectra of the parent 4-OHBP and 4,4'-DiOHBP compounds change slightly their shapes in the spectra of C-4OHBP and C-44DiOHBP. This is indicative of the fact that the parent compounds behave differently in their isolated compound than in the C-4OHBP and C-44DiOHBP. The broad peak in the spectrum of the isolated 4-OHBP is an indication of hydrogen bonding. This broad band assumes two distinct peaks in the spectrum of C-4OHBP. As the two distinct peaks in the spectrum of C-4OHBP are in the same region as in the spectra of 4-OHBP, there are hydrogen bondings in C-4OHBP with the same strength as in the isolated 4-OHBP. However, the hydrogen bonds in C-4OHBP are not expected to be of such a nature as in the case of isolated 4-OHBP, since the peaks in the spectra of C-4OHBP are distinct.

The peak for 4,4'-DiOHBP, in the region 3400 cm^{-1}, becomes broader in the C-44DiOHBP and shifts slightly to higher wavenumber. Broadening of the spectrum of 4,4'-DiOHBP indicates the OH groups result in hydrogen bonds with various strengths. Higher wavenumber of 4,4'-DiOHBP in the spectrum of C-44DiOHBP is an indication of the presence of weaker hydrogen bonds in C-44DiOHBP than in the isolated 4,4'-DiOHBP. At around 3500-3200 cm^{-1}, $\nu_{asym}(NH_2)$ and $\nu_{sym}(NH_2)$ of BZ shift to both higher and lower wavenumbers in the spectrum of C-BZ. This may be because the hydrogens on NH_2-groups can interact differently with their environment, implying hydrogen bonding between NO_2 and NH_2. NH groups generally display much narrower

hydrogen bond stretching than OH-groups, due to the relatively lower electronegativity of NH vis-à-vis OH.

The C-H vibrations of the methyl groups of the NMe_2-group in the C-tmethylbz11 and C-tmethylbz41 occur at the same positions with only intensity variations between the various bands. The same observations can be made for C-4BrBP and C-BP where there seem to be simple combination spectra of their parent compounds. It therefore seems that there is no or little interaction between the individual components of the C-tmethylbz11, C-tmethylbz41, C-4BrBP and C-BP.

Figure 23 The spectra of C-H, N-H and O-H stretches of the parent compounds and their complexes

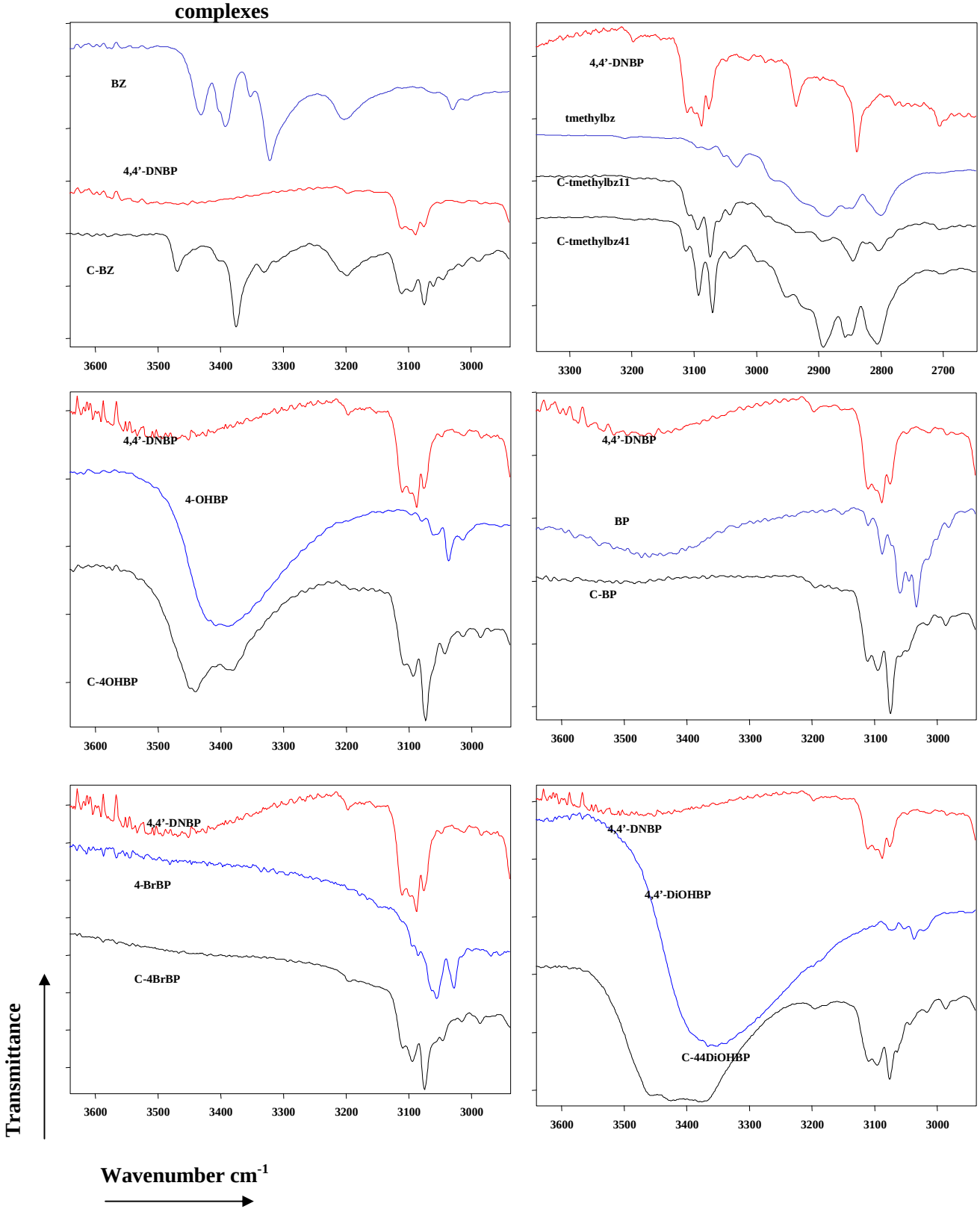

5.3.6 Comparison of spectra of parent components with their molecular complexes

5.3.6.1 C-BZ

Table 22 The vibrational wavenumber values of 4,4'-DNBP, BZ and their complex are given in cm^{-1}

Assignment	4,4'-DNBP		BZ		C-BZ	
	IR	Raman	IR	Raman	IR	Raman
ν_{asy} (NH_2)			3431m		3469w	
			3394m		3375m	
ν_{sym} (NH_2)			3321m		3327w	
2δ (NH_2)			3202w		3196w	
ν_{ring} (CH)					3116w	
ν_{ring} (CH)					3075m	
ν_{ring} (CH)	3088w				3064w	
δ (NH_2)			1627s		1620m	
ν_{ring}	1600s	(1599vs)	1605s	(1607vs)	1594m	(1596s)
ν_{asym} (NO_2)	1511s					
ν_{ring}			1499s		1501s	
ν_{ring}	1477m		1495s			
ν_{ring}				(1448w)		(1454s)
ν_{sym} (NO_2)	1343s	(1344s)			1343 s	
δ (CH)		(1275w)		(1281m)		(1280w)
ν (CN)+ν_{ring}			1262s		1269m	
δ (CH)			1139w			
δ (CH)				(1143m)		(1144vs)
Ring breath	851s		848m	(851m)	850s	
Ring breath	840vs				840 m	
γ_{ring}			749 w		739s	
γ_{ring}			701 m		700w	
γ_{ring}			666 w			

s = strong; m = medium; w = weak; v = very; ν = stretch vibration; ν_{asym} = asymmetric stretch; ν_{sym} = symmetric stretch; δ = deformation; γ = rocking

5.3.6.2 C-tmethylbz11 and C-tmethylbz41

Table 23 The vibrational wavenumber values of 4,4'-DNBP, tmethylbz and their complexes are given in cm^{-1}

Assignment	4,4'-DNBP		tmethylbz		C-tmethylbz11		C-tmethylbz41	
	IR	Raman	IR	Raman	IR	Raman	IR	Raman
ν_{ring}	3088w		3093w		3092w		3094w	
					3070w		3074w	
ν_{ring}			3036w					
			2886m		2942w		2942w	
			2800m		2810w		2806w	
ν_{ring}	1600s	(1599vs)	1611s	(1605vs)	1609s	(1608vs)	1608m	(1601vs)
					1595s		1594m	
ν_{asym} (NO_2)+ν_{ring}	1511s		1508s		1510vs		1508s	
ν_{ring}	1477m							
ν_{ring}			1439m		1442m	(1447m)		(1452s)
ν_{sym} (NO_2)+ν (CN) 3^o amine[48]	1343s	(1344s)	1352s		1338s		1343s	(1348m)
δ_{ring}		(1275w)						
			1164m	(1164vw)	1177s			
						(1145m)		(1144vs)

s = strong; m = medium; w = weak; v = very; ν = stretch vibration; δ = deformation

5.3.6.3 C-4OHBP

Table 24 The vibrational wavenumber values of 4,4'-DNBP, 4-OHBP and their complex are given in cm^{-1}

Assignment	4,4'-DNBP		4-OHBP		C-4OHBP	
	IR	Raman	IR	Raman	IR	Raman
ν (O-H) H-bonded					3440w, br	
ν (O-H) H-bonded			3390m,br		3384w, br	
ν_{ring}	3088w				3074w	
ν_{ring}				(1611m)		
ν_{ring}	1600s	(1599vs)	1597m	(1599vs)	1594m	(1600vs)
			1523m	(1525w)		
ν_{asym} (NO_2)+ν_{ring}	1511s				1508m	
ν_{ring}	1477m		1488m			
ν_{ring}			1425vw			
ν_{sym} (NO_2)	1343s	(1344s)	1376vw		1343s	(1348vs)
δ_{ring}		(1275w)		(1276m)		(1287w)
Ring breath.[Table 20]	851s				850m	(862w)
Ring breath.[Table 20]	840 vs		833m	(832vw)	840m	

s = strong; m = medium; w = weak; v = very; br = broad; ν_{asym} = asymmetric stretch; ν_{sym} = symmetric stretch; δ = deformation

5.3.6.4 C-BP

Table 25 The vibrational wavenumber values of 4,4'-DNBP, BP and their complex are given in cm^{-1}

Assignment	4,4'-DNBP		BP		C-BP	
	IR	Raman	IR	Raman	IR	Raman
ν_{ring}	1600s	(1599vs)	1598w	(1606w)	1595s	(1600vs)
ν_{ring}				(1588w)		
ν_{ring}			1569m			
ν_{asym} (NO_2)	1511s				1509s	
ν_{ring}	1477m		1480s		1478m	
ν_{ring}			1429s		1430w	
ν_{sym} (NO_2)	1343s	(1344s)	1344w		1343vs	(1348vs)
δ_{ring}		(1275w)		(1276m)	1274w	(1274w)
Ring breath.[Table 20]	851s				850s	(862m)
Ring breath.[Table 20]	840vs				840s	
γ_{ring}		(764vw)			751m	(755w)

s = strong; m = medium; w = weak; v = very; ν = stretch vibration; ν_{asym} = asymmetric stretch; ν_{sym} = symmetric stretch; δ = deformation; γ = rocking

5.3.6.5 C-4BrBP

Table 26 The vibrational wavenumber values of 4,4'-DNBP, 4-BrBP and their complex are given in cm^{-1}

Assignment	4,4'-DNBP		4-BrBP		C-4BrBP	
	IR	Raman	IR	Raman	IR	Raman
ν_{ring}	1600s	(1599vs)	1609w	(1595s)	1594s	(1598vs)
ν_{ring}			1582w	(1588vs)		(1583s)
ν_{asym} (NO_2)+ν_{ring}	1511s		1511m		1512s	
ν_{ring}	1477m		1477m		1476s	
ν_{ring}			1448m			(1453w)
ν_{sym} (NO_2)	1343s	(1344s)			1344vs	(1348s)
δ_{ring}		(1275w)	1275vw	(1276m)		(1272m)
Ring breath	851s				850vs	
Ring breath	840s		830vs		838vs	
γ_{ring}			757vs		772m	
γ_{ring}	738s				739vs	

s = strong; m = medium; w = weak; v = very; ν = stretch vibration; ν_{asym} = asymmetric stretch; ν_{sym} = symmetric stretch; δ = deformation; γ = rocking

5.3.6.6 C-44DiOHBP

Table 27 The vibrational wavenumber values of 4,4'-DNBP, 4,4'-DiOHBP and their complex are given in cm^{-1}

Assignment	4,4'-DNBP		4,4'-DiOHBP		Complex7	
	IR	Raman	IR	Raman	IR	Raman
ν_{ring}	1600s	(1599vs)	1610s	(1613vs)		(1600vs)
ν_{ring}			1591s	(1598s)	1594s	
ν_{asym} (NO_2)+ν_{ring}	1511s		1498vs		1505vs	
ν_{ring}	1477m					
ν_{ring}			1424m		1423m	
ν_{sym} (NO_2)	1343s	(1344s)			1344s	(1348vs)
δ (CH)		(1275w)		(1280m)		(1275vw)
			1236s			
				(1190w)		(1193w)
Ring breath	851s			(846w)		
Ring breath	840s					
			818vs			
	738s				738s	

s = strong; m = medium; w = weak; v = very; ν = stretch vibration; ν_{asym} = asymmetric stretch; ν_{sym} = symmetric stretch; δ = deformation; γ = rocking

5.4 Discussion

The infrared and Raman assignments of the parent compounds and those of the complexes were necessary to determine the shifts of parent compounds. The assignments from the literature have been used for correlation.

Interpretation of an infrared spectrum is not a simple matter. Bands may be obscured by overlapping with other bands. Overtones (harmonics) may appear at just twice the frequency of the fundamental band. The absorption band of a particular group may be shifted by various structural features (conjugation, electron withdrawal by a neighbouring substituent, angle strain or Van der Waals strain, hydrogen bonding) and may be mistaken for a band of an entirely different group [28]. The spectral bands show that C-BZ, C-4OHBP and C-44DiOHBP are likely to show hydrogen bonding, whereas C-tmethylbz11, C-tmethylbz41, C-BP and C-4BrBP seem to be stabilised mainly by Van der Waals interactions.

The planar BP and 4,4'-DiOHBP moieties have a centre of symmetry and according to the rule of mutual exclusion, infrared active bands should not be Raman-active or conversely: the Raman-active bands should not be infrared-active. The peaks of both the Raman and infrared spectra of BP and 4,4'-DiOHBP are tabulated, in Table 25 and Table 27, respectively. However, it is clear that the same bands occur in both spectra. The very small non-zero dihedral angle between the two aromatic rings could be responsible for this discrepancy.

In Figure 23, the infrared spectra of C-H, N-H and O-H stretches of the parent compounds and their complexes are shown. The C-H stretches of the components in the complexes appear at higher wavenumbers than for their parent compounds, which indicates that the bond strength of parent compounds has strengthened after complex formation. This strengthening can be ascribed to interactions whose origin may be hydrogen bonding, π-π interaction or the change in the conformation of the components of the complexes. For this reason, infrared and Raman studies do not give significant information with regard to the ring system unless more in depth infrared studies is done on these complexes.

CHAPTER 6 X-Ray Diffraction Studies

6.1 Powder Diffraction

Powder diffraction techniques are used to identify a sample of a solid substance by comparing the relative position of diffraction lines and their intensities with a large diffraction data bank. This data bank is maintained by the International Centre for Diffraction Data Standards (ICDD), and the technique is known as Phase Identification. Powder diffraction data are also used to determine phase diagrams as different solid phases result in different diffraction patterns and to determine the relative amounts of each phase present in a mixture. The technique is also used for the initial determination of the dimensions and symmetries of unit cells and in some cases the crystal structure may also be obtained [23].

In this study this technique is used purely as a fingerprint method and no attempt was made to determine the space group or unit cell parameters.

6.1.1 Experimental

Diffraction data were collected at room temperature on a Siemens D-501 automated diffractometer using a Cu target (λ= 1.5406 Å) operated at 40 kV and 40 mA. The instrument was equipped with a diffracted beam graphite monochromator, divergence slit of 1º, receiving slit of 0.05º and scintillation counter. A sample spinner was used. The sample was step-scanned at 2θ, from 5º to 70º with steps of 0.01º at ψ with a fixed counting time of 1.5 sec at a mean temperature of 25 ºC.

6.1.2 Results

Figure 24 Comparison of the X-ray powder spectra of 4,4'-DNBP, BZ and C-BZ

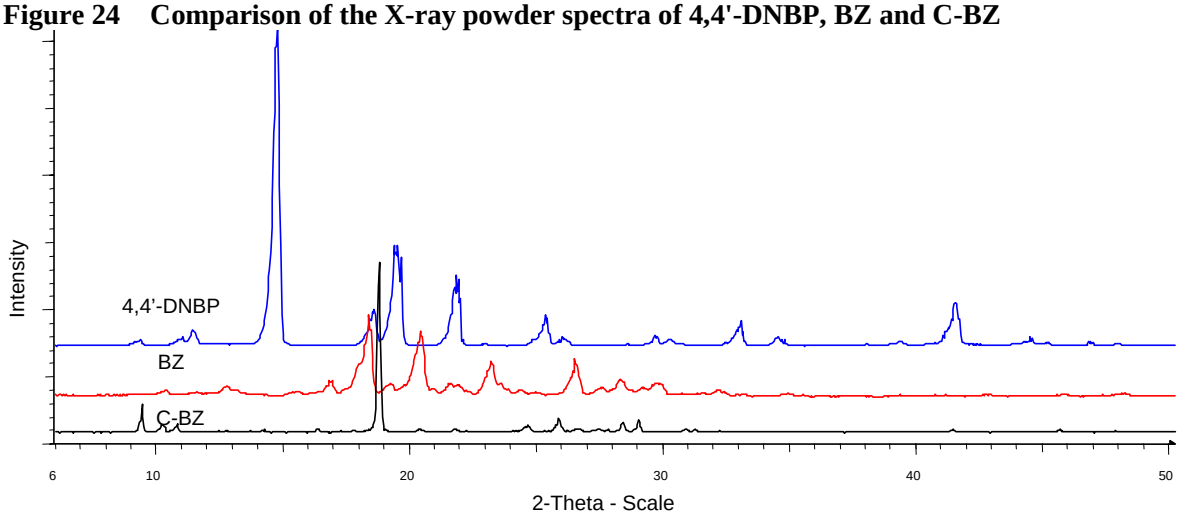

C-BZ has a strong peak at 2θ = 19, where its parent compounds do not show any corresponding peak. The strong peaks of 4,4'-DNBP at 2θ =15 and 22 disappear in the spectrum of C-BZ.

Figure 25 Comparison of the X-ray powder spectra of 4,4'-DNBP and tmethylbz with C-tmethylbz11 and C-tmethylbz41

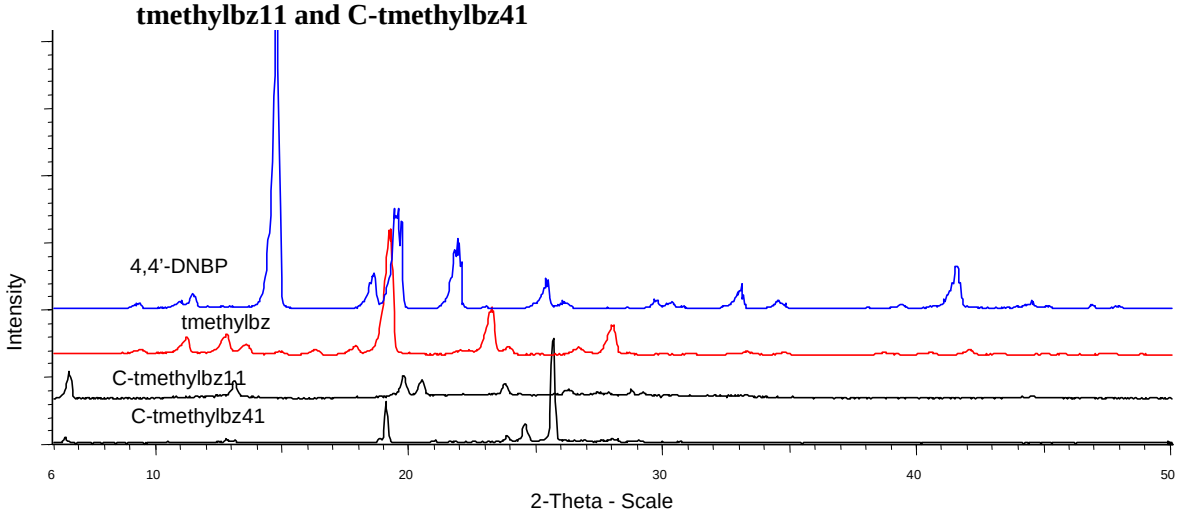

Both C-tmethylbz11 and C-tmethylbz41 have peaks at 2θ ≈ 6.5º, whereas their parent compounds do not have any corresponding peak. The peaks of 4,4'-DNBP at 2θ = 15 and 22º are absent in the complexes. Furthermore, the spectra of

C-tmethylbz11 and C-tmethylbz41 do not match which proves their composition is not the same: C-tmethylbz11 has peaks at 2θ = 20 and 21º, whereas the corresponding peak in C-tmethylbz41 seems to be at 2θ = 19º. The strong peak for C-tmethylbz41 at 2θ = 26º does not appear in C-tmethylbz11. This peak seems to correspond to the peak of 4,4'-DNBP at 2θ = 26º.

Figure 26 Comparison of the X-ray powder spectra of 4,4'-DNBP, 4-OHBP and C-4OHBP

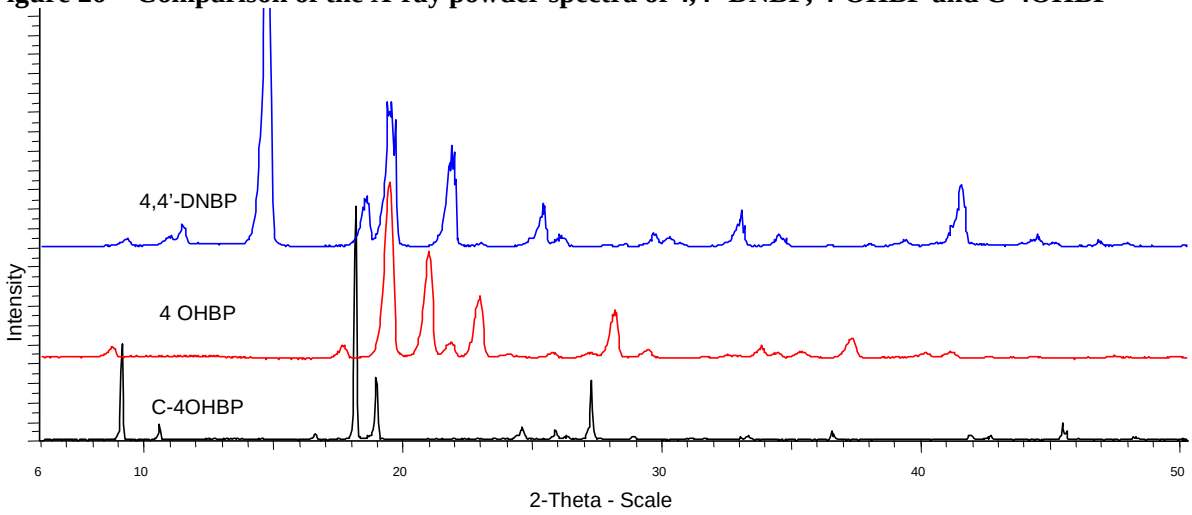

The strong peaks of 4,4'-DNBP at 2θ = 15, 19 and 22º and those of 4-OHBP at 2θ = 19, 22 and 23º disappear in C-4OHBP. Some of isolated 4-OHBP and 4,4'-DNBP compounds seem to shift after the complex formation. For instance, the peaks of C-4OHBP at 2θ = 18º and 19º seem to correspond to the peaks of 4,4'-DNBP at 2θ = 19 and 20 and the peaks of 4-OHBP at 2θ = 19º. A strong peak emerges in C-4OHBP at 2θ = 9º, which may correspond to 4-OHBP.

Figure 27 Comparison of the X-ray powder spectra of 4,4'-DNBP, BP and C-BP

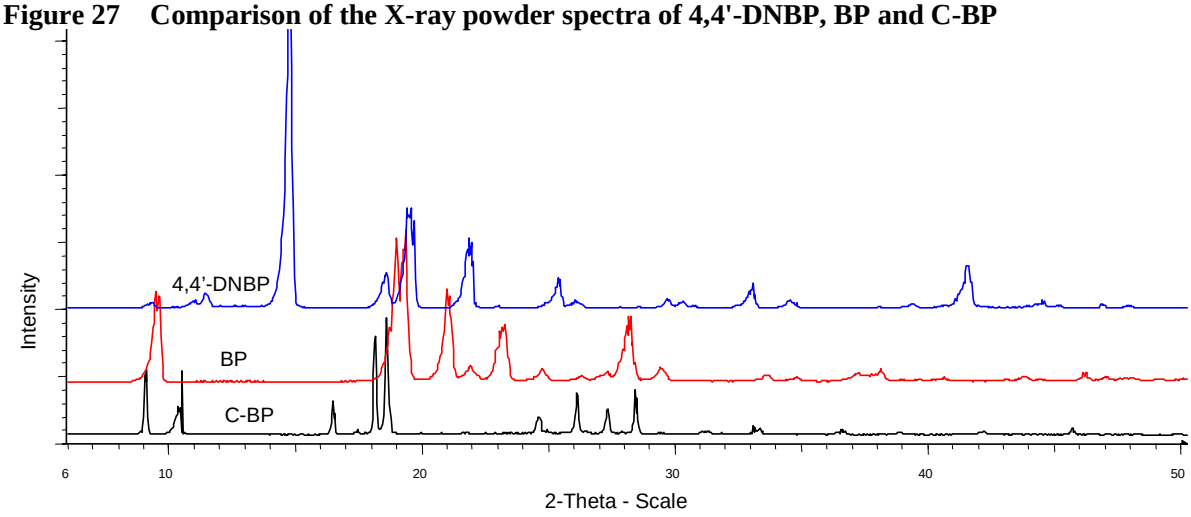

The peaks of 4,4'-DNBP at 2θ = 15 and 22º and the peaks of BP at 2θ = 21 and 23º seem to disappear after the complex formation. Some peaks of the parent compounds seem to shift after the complex formation. For instance, the peaks of C-BP at 2θ = 18 and 19º seem to correspond to the peaks of 4,4'-DNBP at 2θ = 19 and 20 and the broad peak of BP at 2θ = 18-20º. In addition, the peaks of C-BP at 2θ = 9 and 11 seem to correspond to the peak of isolated BP at 2θ = 9.5º.

Figure 28 Comparison of the X-ray powder spectra of 4,4'-DNBP, 4-BrBP and C-4BrBP

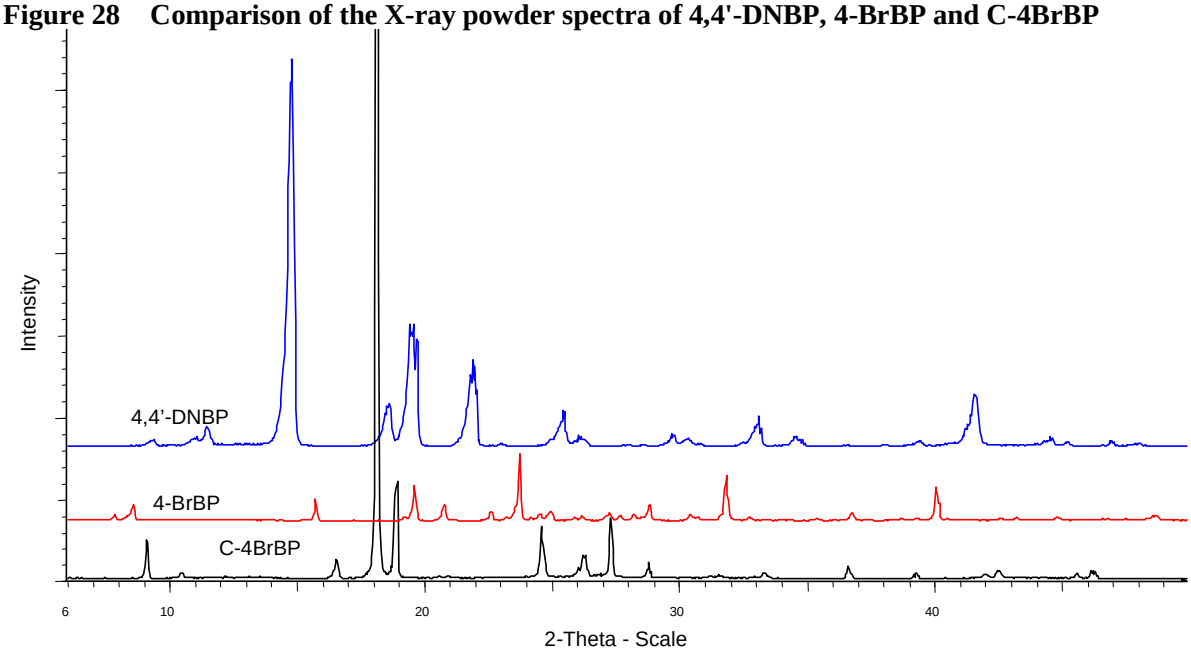

The strong peaks of 4,4'-DNBP at 2θ = 15 and 22º seem to disappear after the complex formation. Some peaks of the parent compounds seem to shift after the complex formation. For instance, the peaks of 4,4'-DNBP at 2θ = 19 and 20º seem to shift that causes the intense diffraction at 2θ = 18º in C-4BrBP.

Figure 29 Comparison of the X-ray powder spectra of 4,4'-DNBP, 4,4'-DiOHBP and C-44DiOHBP

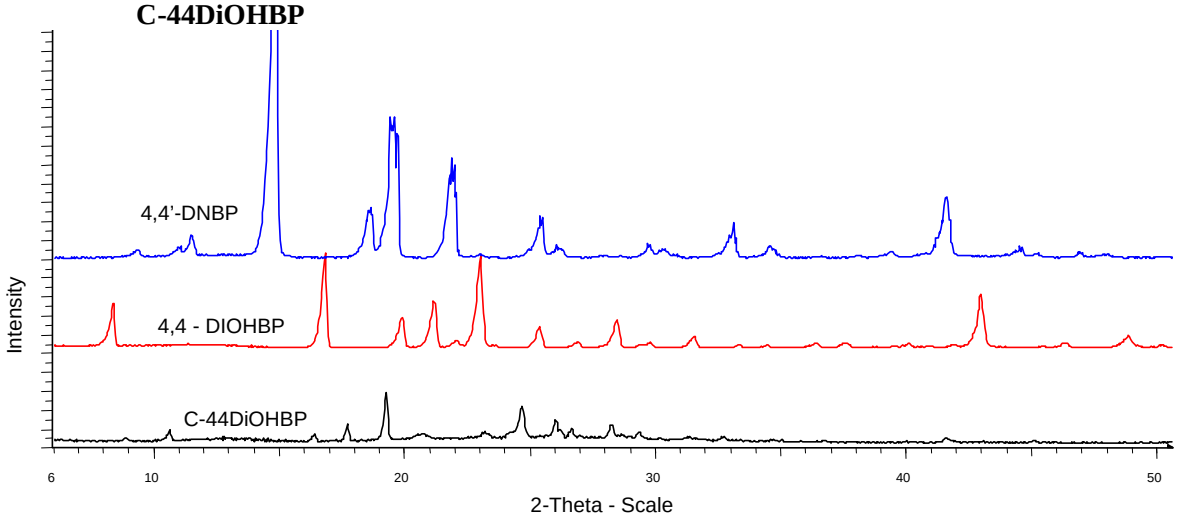

In Figure 29, the strong peaks of 4,4'-DNBP at 2θ = 15 and 22º and those of 4,4'-DiOHBP at

$2\theta \approx 17$ and 23º seem to disappear in the spectrum of C-44DiOHBP.

6.1.3 Discussion

The results show that some strong peaks of parent compounds are absent in the corresponding complexes, conversely new strong peaks are present in the complexes at 2θ values that do not match the peaks present in the parent compounds. This observation suggests that the compounds have reacted to form single crystals of complexes different to that of their parent compounds. However, the detailed changes are in crystallographic character are left unanswered since no attempt was made to make the initial determination of the crystal systems and space groups, or unit cell parameters using powder diffraction technique.

6.2 Single Crystal Structure Determination

C-BZ, C-tmethylbz11, C-tmethylbz41, C-4OHBP, C-BP, C-4BrBP and C-44DiOHBP drew considerable attention in the past due to their intense colours ranging from yellow to dark red, which are dissimilar to the colour combination of their parent compounds. This prompted a series of investigations in the past, but only the structure of C-4OHBP could be obtained by single crystal diffraction [6, 7, 20, 50]. Because the complete structures of the complexes in this study (except C-4OHBP) and the donor compound BZ are not known, their single crystal measurements were attempted.

In this study, the objective is to compare the arrangements and conformations of parent compounds and their changes in the complexes to see if there is any correlation between properties such as dihedral angle and intermolecular distances, with colour formation. Numerous attempts were made to produce suitable diffraction quality crystals of BZ, C-BZ, C-tmethylbz11, C-tmethylbz41, C-BP, C-4BrBP and C-44DiOHBP. Unfortunately, no good diffraction quality crystals could be obtained from these experiments. Although the single crystal structure of 4,4'-DNBP was determined by means of photographic methods by Van Niekerk and Boonstra [1961], the R-factor of this solution was relatively high at 15% [5], which is outside the current internationally accepted standard. As the current technology using automated diffractometers is

much more advanced than the photographic techniques used by Van Niekerk and Boonstra, it was decided to repeat the crystallographic analysis for 4,4'-DNBP. However, despite repeated efforts using a variety of solvents (ethanol, toluene, $CHCl_3$, CH_2Cl_2, benzene, acetonitrile, methyl acrylate, diethyl ether, di-n-butyl ether, ethyl acetate, hexane and acetone:toluene (1:1) mixture) for the crystallisation process in this study, the crystals formed were of a relatively poor quality, resulting in a structure with a similar final R-factor of also approximately 15%. The structure of 4,4'-DNBP could be elucidated, although the data collected were of poor quality, which was the direct result of the poor quality of the available crystals. Figure 30, Figure 31 and Table 28-Table 34 summarise the unit cell parameters determined for 4,4'-DNBP in the present study.

Figure 30 Perspective drawing of 4,4'-DNBP in this study, with numbering scheme used.

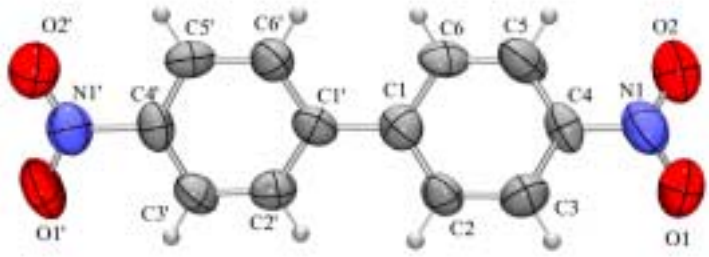

Figure 31 The unit cell drawing of 4,4'-DNBP, viewed along the c-axis.

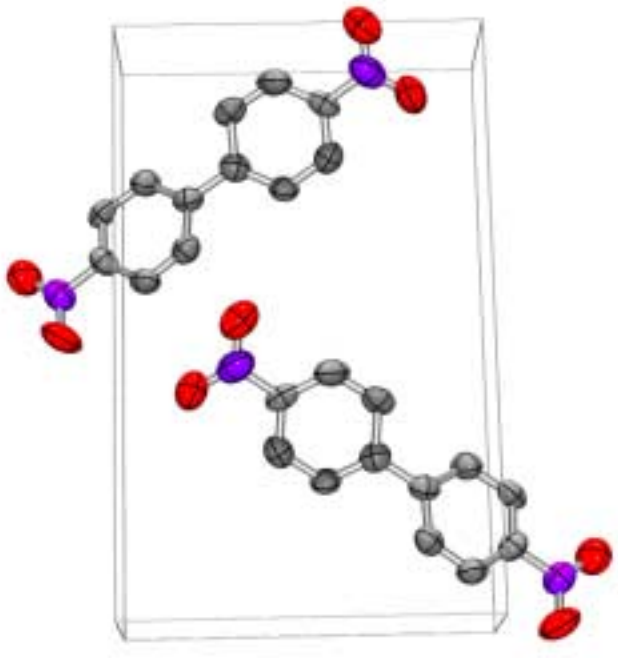

Table 28 Crystal data and structure refinement for 4,4'-DNBP

Identification code	4,4'-DNBP	
Empirical formula	$C_{12}H_8N_2O_4$	
Formula weight	244.20	
Temperature	293(2) K	
Wavelength	0.71073 X	
Crystal system	Monoclinic	
Space group	Pc	
Unit cell dimensions	a = 3.7759(8) X	$\alpha = 90^{O}$.
	b = 9.5907(19) X	$\beta = 90.069(3)^{O}$.
	c = 15.510(3) X	$\gamma = 90^{O}$.
Volume	561.7(2) X^3	
Z	2	
Density (calculated)	1.444 mg/m^3	
Absorption coefficient	0.111 mm^{-1}	
F (000)	252	
Crystal size	0.56 mm x 0.14 mm x 0.12 mm (colourless needles)	
θ range for data collection	2.50 to 26.52 ^{O}.	
Index ranges	$-4 \le h \le 4$, $-6 \le k \le 11$, $-18 \le l \le 15$	
Reflections collected	2929	
Independent reflections	1709 [R (int) = 0.0199]	
Completeness to $\theta = 25^{O}$	99 %	
Refinement method	Full-matrix least-squares on F^2	
Data / restraints / parameters	1709 / 2 / 164	
Goodness-of-fit on F^2	2.317	

Table 28 (continued)

Final R indices [I>2sigma(I)]	R1 = 0.1587, wR2 = 0.4458
R indices (all data)	R1 = 0.1612, wR2 = 0.4506
Absolute structure parameter	4 (6)
Largest diff. peak and hole	0.732 and -0.752 e.X^{-3}

Table 29 **Atomic coordinates (x 10^4) and equivalent isotropic displacement parameters (X^2x 10^3) for 4,4'-DNBP. U(eq) is defined as one third of the trace of the orthogonalized U^{ij} tensor.**

	x	y	z	U(eq)
C (4)	9440(20)	4373(8)	3598(6)	53(2)
C (6)	8990(30)	6878(9)	3527(6)	62(2)
C (2')	6820(30)	8142(8)	1298(6)	58(2)
C (5')	4220(30)	10462(8)	2138(6)	59(2)
C (1')	6470(30)	8068(9)	2186(6)	58(2)
C (4')	4530(20)	10408(8)	1272(6)	57(2)
C (2)	7070(30)	5465(8)	2296(6)	56(2)
C (5)	9740(40)	5677(11)	3965(7)	80(3)
O (1)	9370(40)	1996(9)	3732(7)	106(4)
C (1)	7380(20)	6783(9)	2668(6)	62(2)
C (3')	5900(30)	9265(8)	820(6)	64(2)
O (2)	11880(30)	3296(9)	4752(8)	101(3)
N (1')	3460(30)	11652(9)	765(6)	74(2)
C (6)	5160(30)	9250(9)	2593(7)	64(2)
O (2')	2370(30)	12642(9)	1157(6)	101(3)
O (1')	3970(40)	11590(10)	-6(6)	118(4)
N (1)	10460(30)	3166(11)	4056(7)	87(3)
C (3)	7970(30)	4238(10)	2771(7)	74(3)

Table 30 **Bond lengths [Å] of the non-hydrogen atoms for 4,4'-DNBP**

C (4)-C (5)	1.378 (14)
C (4)-C (3)	1.404 (15)
C (4)-N (1)	1.412 (12)
C (6)-C (5)	1.367 (15)
C (6)-C (1)	1.466 (15)
C (2')-C (3')	1.353 (13)
C (2')-C (1')	1.387 (13)
C (5')-C (4')	1.350 (13)
C (5')-C (6')	1.404 (13)
C (1')-C (6')	1.389 (12)
C (1')-C (1)	1.481 (12)
C (4')-C (3')	1.400 (13)
C (4')-N (1')	1.484 (11)

Table 30 (continued)

C (2)-C (1)	1.394 (12)
C (2)-C (3)	1.430 (14)
O (1)-N (1)	1.296 (16)
O (2)-N (1)	1.210 (16)
N (1')-O (2')	1.201 (13)
N (1')-O (1')	1.214 (14)

Table 31 Bond angles [º] of the non-hydrogen atoms for 4,4'-DNBP

C (5)-C (4)-C (3)	119.6 (8)
C (5)-C (4)-N (1)	120.9 (9)
C (3)-C (4)-N (1)	119.4 (9)
C (5)-C (6)-C (1)	119.0 (8)
C (3')-C (2')-C (1')	124.1 (8)
C (4')-C (5')-C (6')	116.5 (7)
C (2')-C (1')-C (6')	116.3 (8)
C (2')-C (1')-C (1)	121.4 (7)
C (6')-C (1')-C (1)	122.2 (8)
C (5')-C (4')-C (3')	124.1 (8)
C (5')-C (4')-N (1')	118.2 (8)
C (3')-C (4')-N (1')	117.7 (8)
C (1)-C (2)-C (3)	120.9 (8)
C (6)-C (5)-C (4)	122.8 (9)
C (2)-C (1)-C (6)	117.8 (8)
C (2)-C (1)-C (1')	121.7 (8)
C (6)-C (1)-C (1')	120.2 (8)
C (2')-C (3')-C (4')	116.4 (8)
O (2')-N (1')-O (1')	126.3 (9)
O (2')-N (1')-C (4')	117.5 (9)
O (1')-N (1')-C (4')	116.0 (9)
C (1')-C (6')-C (5')	122.5 (9)
O (2)-N (1)-O (1)	125.1 (10)
O (2)-N (1)-C (4)	119.0 (10)
O (1)-N (1)-C (4)	115.3 (11)
C (4)-C (3)-C (2)	119.2 (8)

Table 32 **Anisotropic displacement parameters (X^2x 10^3)for 4,4'-DNBP. The anisotropic displacement factor exponent takes the form: $-2\pi^2[h^2a^{*2}U^{11} + ... + 2 h k a^* b^* U^{12}]$**

	U^{11}	U^{22}	U^{33}	U^{23}	U^{13}	U^{12}
C (4)	31(3)	71(4)	58(5)	19(3)	2(3)	3(3)
C (6)	64(5)	70(4)	53(5)	-14(3)	25(4)	-11(4)
C (2')	54(4)	63(4)	58(5)	-4(3)	1(4)	-9(3)
C (5')	59(5)	63(4)	55(5)	-15(3)	10(4)	-9(3)
C (1')	56(5)	67(4)	49(4)	-5(3)	-3(4)	-5(3)
C (4')	48(4)	64(4)	58(5)	14(3)	-10(3)	-3(3)
C (2)	53(4)	62(4)	53(4)	2(3)	-10(4)	-3(3)
C (5)	95(9)	97(7)	48(5)	2(4)	-17(5)	-12(5)
O (1)	143(10)	76(4)	100(7)	9(4)	-2(7)	14(5)
C (1)	54(5)	68(5)	63(5)	-2(3)	4(4)	8(3)
C (3')	74(6)	69(4)	48(4)	8(3)	3(4)	-8(4)
O (2)	93(7)	104(6)	106(7)	29(5)	-14(6)	8(5)
N (1')	71(6)	78(5)	74(6)	12(4)	-4(5)	-11(4)
C (6')	63(5)	74(5)	56(5)	-3(3)	-5(4)	17(4)
O (2')	112(7)	94(5)	98(6)	6(5)	-3(5)	22(5)
O (1')	162(11)	120(7)	73(6)	37(5)	-7(7)	33(7)
N (1)	91(8)	102(8)	68(6)	18(4)	9(5)	11(5)
C (3)	84(8)	62(4)	75(7)	-8(4)	-8(6)	-13(4)

Table 33 **Hydrogen coordinates (x 10^4) and isotropic displacement parameters (X^2x 10^3 for 4,4'-DNBP**

	x	y	z	U(eq)
H (6)	9494	7742	3770	80(11)
H (2')	7737	7370	1012	80(11)
H (5')	3433	11260	2419	80(11)
H (2)	6258	5384	1732	80(11)
H (5)	10488	5742	4535	80(11)
H (3')	6162	9278	224	80(11)
H (6')	4888	9239	3189	80(11)
H (3)	7587	3359	2534	80(11)

Table 34 Dihedral angles [°] of the non-hydrogen atoms for 4,4'-DNBP

C (3')-C (2')-C (1')-C (6')	-1.3 (14)
C (3')-C (2')-C (1')-C (1)	177.3 (10)
C (6')-C (5')-C (4')-C (3')	-3.8 (14)
C (6')-C (5')-C (4')-N (1')	178.0 (9)
C (1)-C (6)-C (5)-C (4)	7.8 (18)
C (3)-C (4)-C (5)-C (6)	-6.6 (19)
N (1)-C (4)-C (5)-C (6)	175.9 (12)
C (3)-C (2)-C (1)-C (6)	5.9 (14)
C (3)-C (2)-C (1)-C (1')	179.8 (10)
C (5)-C (6)-C (1)-C (2)	-7.3 (14)
C (5)-C (6)-C (1)-C (1')	178.7 (10)
C (2')-C (1')-C (1)-C (2)	-29.5 (14)
C (6')-C (1')-C (1)-C (2)	149.0 (10)
C (2')-C (1')-C (1)-C (6)	144.2 (9)
C (6')-C (1')-C (1)-C (6)	-37.2 (14)
C (1')-C (2')-C (3')-C (4')	0.2 (14)
C (5')-C (4')-C (3')-C (2')	2.6 (15)
N (1')-C (4')-C (3')-C (2')	-179.3 (9)
C (5')-C (4')-N (1')-O (2')	-0.1 (14)
C (3')-C (4')-N (1')-O (2')	-178.4 (10)
C (5')-C (4')-N (1')-O (1')	176.1 (11)
C (3')-C (4')-N (1')-O (1')	-2.2 (15)
C (2')-C (1')-C (6')-C (5')	-0.1 (15)
C (1)-C (1')-C (6')-C (5')	-178.7 (9)
C (4')-C (5')-C (6')-C (1')	2.5 (15)
C (5)-C (4)-N (1)-O (2)	-5.9 (17)
C (3)-C (4)-N (1)-O (2)	176.6 (11)
C (5)-C (4)-N (1)-O (1)	165.7 (12)
C (3)-C (4)-N (1)-O (1)	-11.8 (15)
C (5)-C (4)-C (3)-C (2)	4.9 (16)
N (1)-C (4)-C (3)-C (2)	-177.6 (11)
C (1)-C (2)-C (3)-C (4)	-4.8 (16)

6.2.1 Literature

The Cambridge Structural Database (CSD) was used for the literature search. The CSD is the internationally recognised depository for single crystal structure data as it is fully retrospective, updated on a regular basis and all information is abstracted from primary journals and associated supplementary information in both hard copy and electronic forms. The CSD was therefore used to obtain crystallographic data for the parent compounds and molecular complexes investigated in this study [51].

6.2.1.1 Background to the single crystal structure determinations of some compounds of importance to this study

Table 35 is not aimed at showing all the possible single crystal records of compounds, but to show only some details of the best single crystal studies to date of all the parent compounds and the complexes in this study. There is no information available on BZ, C-BZ, C-tmethylbz11, C-tmethylbz41, C-BP, C-4BrBP and C-44DiOHBP in the CSD resources.

Table 35 Some relevant structure determination

Compounds	Temperature	R-factor (%)	Year	References
4,4'-DNBP	RT	15.0	1963	Boonstra [17]
tmethylbz	RT	5.4	1988	Nakai, Saito, Yamakawa [52]
4-OHBP	RT	4.2	1984	Brock, Haller [53]
BP	RT	6.3	1977	Charbonneau, Delugeard [54]
4-BrBP	152K	5.0	1980	Brock [55]
4,4'-DiOHBP	RT	3.7	1990	Jackish, Fronczek, Geiger [56]
C-4OHBP	RT	6.2	1984	Brock, Haller [57]

6.2.2 Discussion

In Table 36, a list of dihedral angles of the individual parent compounds is presented in an attempt to assess whether there is a correlation between the electronic properties of their substituents with the twist that occurs in the central sigma bond of the BP rings. There is no information about the BZ molecule, which is a donor compound. Although the substituents of tmethlbz, 4-OHBP and 4,4'-DiOHBP are electron-donor, they differ from each other in that 4-OHBP and 4,4'-DiOHBP are planar, whereas tmethylbz is non-planar. On the other hand, the electron-withdrawing substituted compounds, 4,4'-DNBP and 4-BrBP are non-planar. The following model can be suggested: it may be possible that the electron-donor substituted compounds favour planarity, and electron-withdrawing substituted compounds favour non-planarity. Based on this, the non-planarity of an electron-donor compound such as tmethylbz could be explained as resulting from steric interactions. However, no supportive proof has been obtained using the CSD search on the following compounds, which were the only small BP molecule (except the molecules in this study) in the CSD: 4,4'-difluorobiphenyl, 4,4'-dichlorobiphenyl, 4-bromo-4-fluorobiphenyl, 4-bromo-4-chlorobiphenyl. These substituents on these molecules differ electronically from each other, such that 4,4'-difluorobiphenyl should be

more electron-withdrawing due to the high electronegativity of the fluoro substituent. However, there is no correlation between the increase or decrease in their dihedral angles with regard to the substituents that BP takes on its *para* positions.

Table 36 Dihedral angles of the parent compounds in the central C-C bond of their biphenyl rings

Parent compounds	**Dihedral angle in the central C-C bond of the biphenyl rings in the parent compounds**
4,4'-DNBP	39.6 (non-planar)
tmethylbz	13.8 (non- planar)
4-OHBP	2.5 and 2.8 (planar)
BP	1.0 (planar)
4-BrBP	15.6 and 24.4 (non-planar)
4,4'-DiOHBP	0.3 (planar)

The coordinates of only one complex in this study (C-4OHBP) are available in the literature. In Table 37, the central sigma bonds of the aromatic rings of C-4OHBP have been compared with those of its parent compounds to assess whether the complex formation favours the planarity of the components within the complex. Table 37 shows that the components assume a more planar orientation in C-4OHBP than in the parent compounds. However, this is not a significant change and therefore this information does not account for the relative planarity of the compounds in the other complexes in this study.

Table 37 Comparison of planarity of the parent compounds of 4,4'-DNBP and 4-OHBP with the components of the C-4OHBP

Dihedral angle of the aromatic rings	**4,4'-DNBP**	**4-OHBP**	**C-4OHBP**	
			4,4'-DNBP component	**4-OHBP component**
Central C-C bond of the biphenyl rings	39.6	2.5 and 2.8	36.7	0.4

The physical properties of the parent compounds have been analysed to obtain information about the forces that predominate. Hunter and Sanders suggested a model that permits the prediction of physical properties on condition that the molecules have π–π interactions [8]. This model considers π–π interaction as an interaction whose main components are Van der Waals and electrostatic forces instead of charge transfer. The model works for a variety of compounds but a main drawback results from the fact that it ignores the short-range effects (such as hydrogen

bonding) and induction [8, 9]. The key feature of the model is that the σ framework and the π electrons are considered separately and the net favourable σ-π interactions are actually the result of interactions that overcome π-π repulsions. The model predicts that for nonpolarised π systems, π–π repulsion dominates in a face-to-face π-stacked geometry, σ-π interaction dominates in an edge-on (T-shaped geometry) or σ-π interaction dominates in an offset (slip between the two π-systems that belong to an adjacent molecule) π-stacked geometry [8]. For neutral atoms in this geometry the dominant interaction is π-electron repulsion, so that an atom which is π-deficient stabilises the interaction by decreasing the repulsion. Conversely, a π-rich atom would destabilise the interaction further. When both atoms are strongly charged, the obvious result is obtained: like polarizations repel and unlike polarisations attract. This implies that when the rings have electron-donating substituents, the rings will be π-rich and thus electrostatic interaction between the rings in a face-to-face geometry is not favourable for π-π interaction: therefore σ-π interaction dominates and leads to a 90° orientation or offset π-stacked geometry [8]. Conversely, when the rings are substituted with electron-withdrawing groups, π–π repulsion will predominate resulting in a face-to-face geometry [8]. As the electron-withdrawing substituents favoured a face-to-face geometry, it was expected that 4,4'-DNBP and 4-BrBP have a similar geometry. Similarly, electron-donor group substituted BZ, tmethylbz, 4-OHBP and 4,4'-DiOHBP were expected to show σ-π interactions that favour a 90° orientation or offset π-stacked geometry. The geometry of these parent compounds has been analysed and explained later in detail under three subtitles: BP compound without substituents (BP), BP compounds with electron-withdrawing substituents (4,4'-DNBP and 4-BrBP), and BP compounds with electron-donating substituents (BZ, tmethylbz, 4-OHBP and 4,4'-DiOHBP). Not all the compounds fitted the model. The anomaly in the geometrical arrangements of the molecules that have small intermolecular distances between the neighbouring aromatic rings may be interpreted in terms of the effect of short contacts and inductions that predominate the factors that the model relies on.

6.2.2.1 BP compound without substituents (BP)

Figure 32 A view of the molecular packing of BP, showing the parallel layers of BP molecules

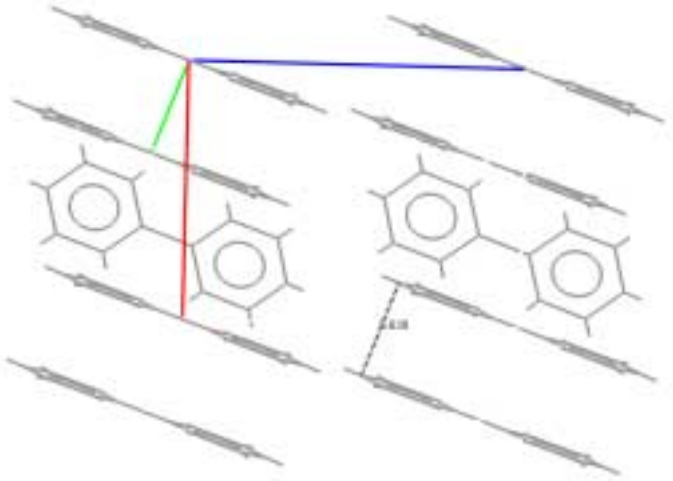

A face-to-face π-stacked geometry. The distance between consecutive parallel layers is approximately **5.6 Å.**

In Figure 32, the BP molecules are layered parallel to each other in a face-to-face π-stacked geometry with a distance of 5.6 Å between the neighbouring layers. This distance between the aromatic rings is considered too far for any electrostatic interaction. No hydrogen bonding and short contact has been observed in the CSD data. Therefore it seems that if any force exists at all, it should be very weak. This is reflected in the relatively low melting point (67ºC) of BP.

6.2.2.2 BP compounds with electron-withdrawing substituents (4-BrBP and 4,4'-DNBP)

Figure 33 A view of the molecular packing of 4-BrBP, showing the parallel layers of 4-BrBP molecules

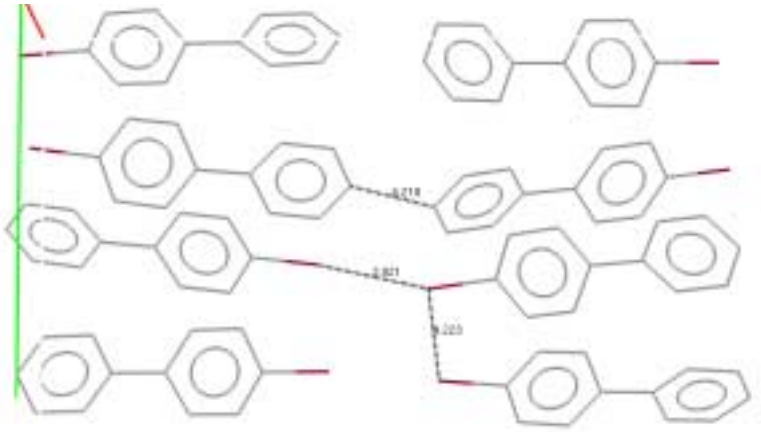

An offset π-stacked geometry. The distance between consecutive layers is approximately **3.7 Å.**

The crystal structure of 4-BrBP has two asymmetric units in the unit cell, with no hydrogen bonding or short contact. The neighbouring aromatic rings are within the expected distance for π-π interaction. This results in a melting point of 87ºC, which is slightly higher than that observed for BP. As 4-BrBP has a Br atom which is a slightly electron-withdrawing substituent, a face-to-face geometry would be expected. But instead an offset π-stacked geometry has been observed. This is most likely due to the polarity and size of the Br atom which may interact with the nearest aromatic ring.

Figure 34 A view of the molecular packing of 4,4'-DNBP, showing the parallel layers of 4,4'-DNBP molecules

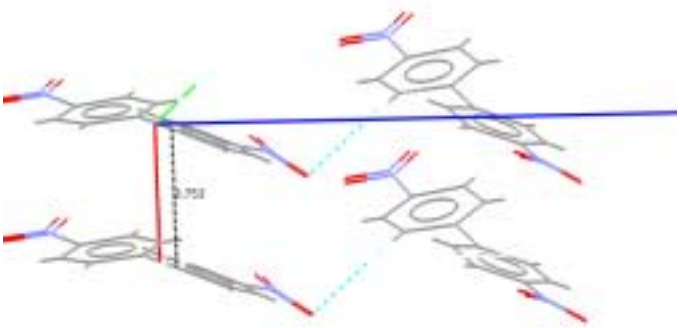

A face-to-face π-stacked geometry. The distance between consecutive parallel layers is approximately **3.7 Å**

The 4,4'-DNBP crystal structure in Figure 34 shows that the molecules have a non-planar dihedral angle around the central C-C bond of the BP rings. The molecules are stacked with the aromatic rings face-to-face in parallel layers with the distance of 3.7 Å between layers. This relatively short distance, compared to the BP layers, leads to the favourable electrostatic interaction for the biphenyl molecules with electron-withdrawing substituents on their ring, which is a face-to-face π-stacked geometry. The electrostatic interaction and van der Waals forces, the main components of π–π interactions, increase the intermolecular attraction between the molecules, which results in the very high melting point (235ºC) relative to that of BP.

6.2.2.3 BP compounds with electron-donating substituents

Figure 35 A view of the molecular packing of tmethylbz, showing the parallel layers of tmethylbz molecules

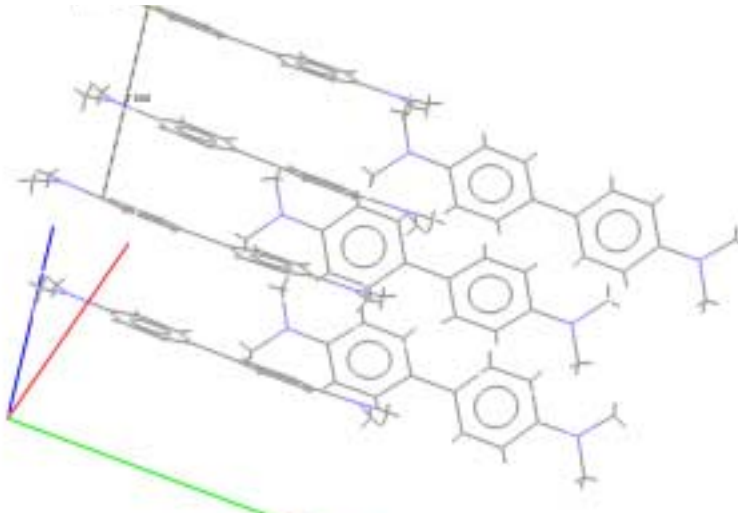

An offset π-stacked geometry. The distance between consecutive parallel layers is approximately **3.7 Å**

In the tmethylbz crystal structure (Figure 35), the presence of the donor substituents on the aromatic rings leads to π–σ interaction with the consecutive adjacent parallel tmethylbz molecules. The molecules are in parallel layers but each time slipped (offset) so that the electron-rich aromatic rings of the one molecule overlap with the more positive C-C central bond of the BP rings of the adjacent molecule. The distance between the neighbouring planes is 3.7 Å, which is similar to that of 4,4'-DNBP and suggests dominating π-π interaction. This staggered geometry is in accordance with the preferred geometry for electrostatic interactions [8], for the aromatic rings with electron-donating substituents. In this molecule, no hydrogen bonding or close

contacts were observed. The relatively high melting point of 189°C is attributed mainly to electrostatic interactions and Van der Waals forces (π–π interaction).

Figure 36 A view of the molecular packing of 4-OHBP, showing the parallel layers of 4-OHBP molecules

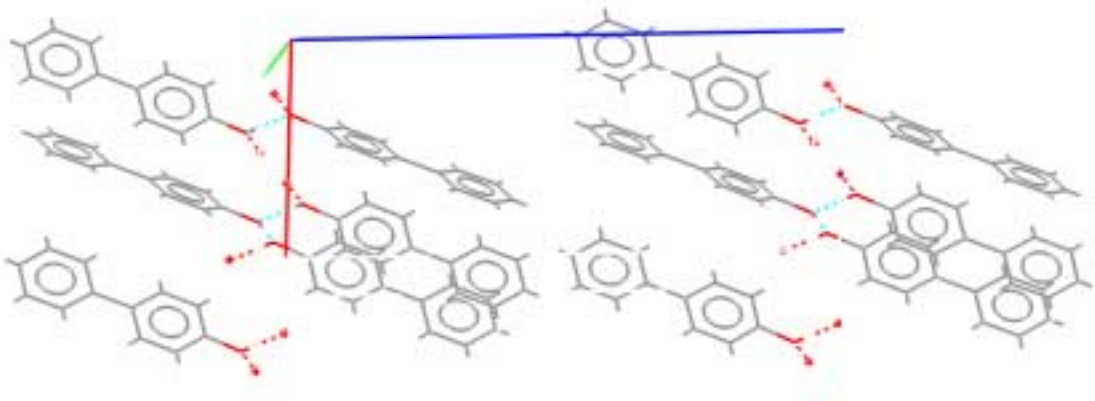

An offset π-stacked geometry. The distance between consecutive parallel layers is approximately 4.7 **Å**

The distance between the neighbouring parallel planes is 4.7 Å. The neighbouring aromatic rings are outside the expected distance for interaction. Therefore, electrostatic interaction (π-σ interaction) is not expected. Hydrogen bonding and short contacts are observed between oxygen atoms and hydrogen atom of the neighbouring OH groups. The extensive network of hydrogen bonds may explain the relatively high melting point of 161°C.

Figure 37 A view of the molecular packing of 4,4'-DiOHBP, showing the parallel layers of 4,4'-DiOHBP molecules

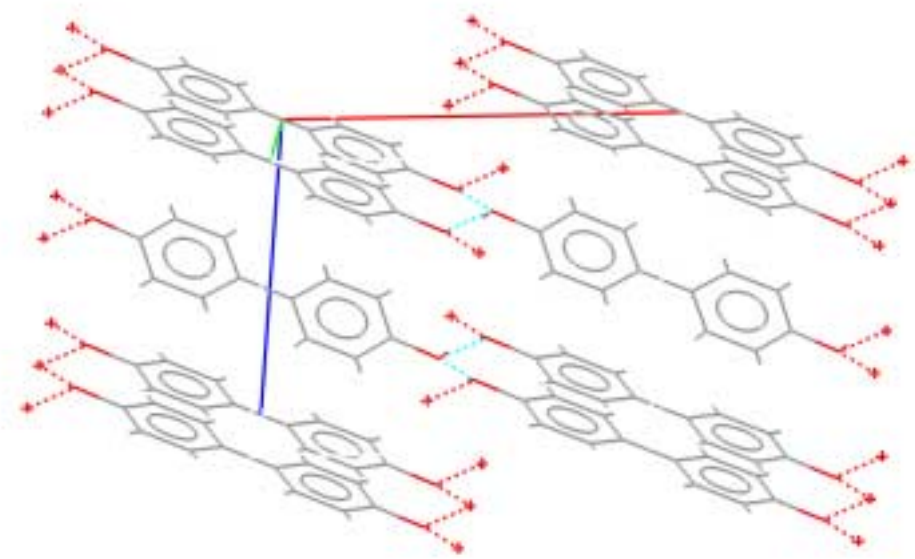

Face-to-face arrangement. The distance between consecutive parallel layers is approximately 3.6 Å

The 4,4'-DiOHBP molecules are stacked in a face-to-face arrangement. The electron-donor substituted biphenyl compounds were supposed to be an offset π-stacked geometry if the electrostatic and Van der Waals forces are predominant, but 4,4'-DiOHBP appears to show face-to-face π-stacked geometry, although the rings have electron-donor substituents. This can be attributed to the fact that the major contribution to the interaction energy in 4,4'-DiOHBP comes from another interaction rather than van der Waals and the electrostatic forces: this interaction is most likely hydrogen bonding, as observed in the CSD. But, the extensive network of chains of hydrogen bonding may explain the high melting point of 239°C.

There is no data available about the BZ molecule and its geometrical arrangement is also hard to predict. On the one hand, BZ is expected to show π–σ attraction that dominates in an offset π-stacked geometry (as in the case for tmethylbz and 4-OHBP) for it has donor substituents but on the other hand its substituents also have the ability to form hydrogen bonds as in the case of 4,4'-DiOHBP. Yet the melting point of BZ is relatively low (123ºC). For this reason, it may be suggested that the structure is not dominated by hydrogen bonding.

CHAPTER 7 Conductivity measurements

7.1 Introduction

It is known that two (or more) organic compounds with complementary π-electron or hydrogen bonding acceptor/donor properties can self-assemble, leading to the formation of supramolecular species [58, 59]. The formation of deeply coloured molecular compounds from quinones and nitro compounds on the one hand, and certain unsaturated hydrocarbons and their derivatives on the other hand, has been attributed (Weiss, 1942) [7] to a complex molecule, essentially ionic in character, which is formed from the two components by an electron transfer from the unsaturated hydrocarbon (or its derivative) (donor A), to the polynitro-compound (acceptor B) according to the reaction $A+B=>[A]^{+}\ [B]^{-}$. This postulate of an integral electron transfer from A to B can be regarded as possibly valid only in the limiting case: there should be deep colouring that accompanies molecular complex formation and the presence of ions or ion pairs should be supported by other evidence [7].

Another theory is that molecular complexes can be formed by partial or complete electron transfer between the excited states of the components, giving molecular complexes with non-ionic ground states (Mulliken compounds) [3].

It was a requirement to assess the possible charge transfer in the complexes and their parent compounds in this study. Such species can be considered coordination compounds since their formation is similar to that of metal complexes as it leads to a much higher degree of organization than if there were only Van der Waals forces which cause predictable changes in several properties. Two different methods are used for this purpose; namely: cyclic voltammetry and electric conductivity. The difference between these methods used in this study is the medium of operation. Cyclic voltammetry measurements have been operated in solution, whereas electrical conductivity measurements are carried out in the solid phase.

7.2 Cyclic Voltammetry

Cyclic voltammograms trace the transfer of electrons during an oxidation-reduction (redox) reaction. The reaction begins at a certain potential (voltage). As the potential changes, it controls the point at which the redox reaction will take place. Electrodes are placed in an electrolyte solution. The electrolyte contains the analyte that will undergo a redox reaction [60]. The basic shape of the current response for a cyclic voltammetry experiment is shown below in Figure 38 [61].

Figure 38 Current response for a typical cyclic voltammetry experiment

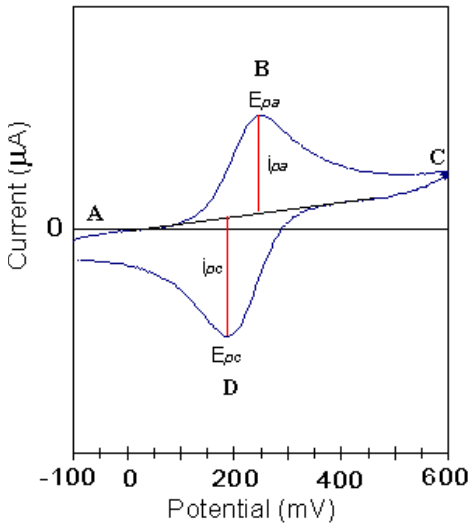

This method was used in this study, as it was necessary to know the electroactivity of compounds and whether charge transfer played any role in the formation of complexes.

7.2.1 Experimental

Cyclic voltammetric measurements were performed in 0.1M solutions of acetone with Pt counter (indicator) electrode, glassy carbon working electrode and Ag/AgCl reference electrode at a scan speed of 5 mVs^{-1} and 50 mVs^{-1}, using 663 VA Stand METROHM and 4.9 GPES Manager.

7.2.2 Results

None of the cyclic voltamograms of the compounds showed any current response. This indicates that no reversible oxidation-reduction reaction of any compound occurs. There is no charge transfer in any of the parent compounds and molecular complexes when they are in solution.

7.3 Electrical Conductivity

7.3.1 Experimental

Pellets of thickness 0.022-0.05 cm were pressed at $5x10^{7}$ Pa. Electrical current-voltage measurements were done, using a HP4140B pico ammeter/DC voltage source with a lowest detection limit of 10^{-13}-10^{-14} Amp. The measurements were done in the dark at 1V, 10V and 100V, respectively. Current measurements below 10^{-14} A were not reliable.

7.3.2 Results

tmethylbz at 1V $1.22*10^{-13}$A
at 10V $1.17*10^{-12}$A
at 100V $1.14*10^{-11}$A
at –1V $5.28*10^{-13}$A
at –10V $-1.09*10^{-12}$A

All the other current measurements of parent compounds and a current flow of the complexes show less than 10^{-14}A.

7.4 Discussion

The electrical conductivity method where the solid states of both parent compounds and complexes are investigated is a good option for the type of problems occurring in solution. Complexes were not affected by solvent interactions and did not dissociate into their components.

As all the experiments were operated in the dark, the light-sensitive parent compound BZ did not decompose either.

Current is detected only in the sample of tmethylbz. However, its complexes did not show any current flow. This is attributed to closer arrangement of the components and their tilting in the complex, which prevented electron flow from passing through the gaps within these complexes (Figure 39).

Figure 39 Electron flow in the idealised complex

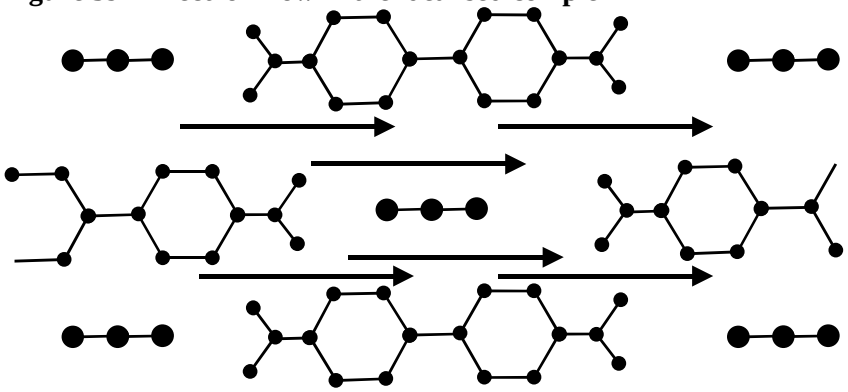

No current flow was observed in cyclic voltammetry. Even the tmethylbz which showed current flow in electric conductivity measurements in the solid state failed to show any current flow. This may be attributed to the fact that tmethylbz may have a different conformation in solution, like some other biphenyls mentioned earlier. In this regard, it is not evident whether a charge transfer caused the complex formation, since the overall geometry of the complex can prevent the observation of charge transfer, although it may exist.

Weak hydrogen bonding, if it exists, cannot be observed with conductivity measurements, since ion formation results in a strong hydrogen bonding.

RECOMMENDATIONS

In this study, none of the complexes or parent compounds produced an acceptable quality single crystals, and as such X-ray crystal structure determination of the complexes could not be done. The use of powder data for structure refinement (Rietveld methods) may be an alternative method to determine the structures of the complexes. Besides, on the basis that biphenyls have a low barrier of rotation around the central bond, one could attempt to make structural and spectroscopic studies at a lower temperature. Equipment to obtain low temperature data was not readily available.

No charge transfer was observed in either the parent compounds or molecular complexes of this study. It is hardly possible to relate the strong colouring to better conjugation of the components of molecular complexes on the basis that the components of C-4OHBP gain better conjugation following the directions of the previous X-ray studies of this complex. IR and Raman spectra do not show mutual exclusion for nonsymmetric compounds such as, 4-OHBP and 4-BrBP since they can never be centrosymmetric, although they may be planar. IR and Raman studies could obtain no information about the planarity of compounds. Therefore, the conjugation question is left unanswered unless more detailed solid state structural and spectroscopic measurements are done.

The future preparations of complexes should involve the molecular ratios determined in the present study using the NMR results. This will lead to better crystals and could be used for the refinement of single crystal measurements.

The π–π interactions model developed by Hunter and Sanders may be used to estimate the bonding properties of the complexes of 4,4'-DNBP. This model offers a sound theoretical basis and provides a powerful insight into the origins of aromatic-aromatic interactions [8].

REFERENCES

1 Bolton, B. and Prasad P.N., *Chem. Phys.*, 1978, **32**, 403-417

2 Morokuma, K., *Acct. Chem. Res.*, 1977, **10**, 295

3 Herbstein, F.H., *Perspectives in Structural Chemistry*, 1971, **4**, 166-184

4 Mulliken, R.S., *J. Am. Chem. Soc.*, 1952, **72**, 600

5 van Niekerk, J.N., Boonstra, E.G., *Acta Cryst.*, 1961, **14**, 1186

6 van Niekerk, J.N. and Saunder, D.H., *Acta Cryst.*, 1948, **1**, 44

7 Rapson, W.S., Saunder, D.H. and Stewart E.T., *J. Chem. Soc.*, 1946, 1110

8 Hunter, C.A. and Sanders, J.K.M, *J. Am. Chem. Soc.*, 1990, **112**, 5525-5534

9 Askew, B., Ballester, P., Buhr, C., Jeong, K.S., Jones, S., Parris, K., Williams, K., Rebek, J., *J. Am. Chem. Soc.*, 1989, **111**, 1082-1090

10 Kuroboshi, M., Waki, Y. and Tanaka, H., *SYNLETT*, 2002, **4**, 637-639

11 Levit, P.B., Belyakov, A.V. and Tselinskii, I.V., *J. Mol. Struct.*, 1992, **265**, 329-336

12 Domenicano, A. and Murray-Rust, P., *Tetrahedron Lett.*, 1979, **24**, 2283

13 Norrestam, R. and Schepper, L., *Acta Chem. Scand. Ser. A*, 1981,**35**, 91

14 Domenicano, A., Vaciago, A. and Coulson, C.A., *Acta Cryst.*, 1975, **B31**, 221

15 Almenningen, A., Bastiansen, O., Gundersen, S, Samdal, S. and Skancke, A., *J. Mol. Struct.*, 1985, **128**, 95

16 Almenningen, A, Bastiansen, O., Fernholt, L., Gundersen, S., Kloster-Jensen, E., Cyvin, B.N., Cyvin, S.J., Samdal, S. and Skancke, A., *J. Mol. Struct.*, 1985, **128**, 77

17 Boonstra, E.G., *Acta Cryst.*, 1963, **16**, 816

18 Herbstein, F.H. and Schoening, F.R.L., *Acta Cryst.*, 1957, **10**, 657

19 Kitaigorodskii, A.I., *Soviet Phys. Cryst.*, 1958, **3**, 393

20 Saunder, D.H., *Proc. Roy. Soc.*, 1947, **A190**, 518

21 Abe, K., Matsunga, Y. and Saito G., *Bull. Chem. Soc. Japan*, 1968, **41**, 2852

22 Nakamoto, K., *Bull. Chem. Soc. Japan*, 1953, **26**, 70

23 Atkins, P.W., *Physical Chemistry*, 5th Ed., Oxford University Press, 1994, 625-728

24 Robinson, J.W., *Undergraduate Instrumental Analysis*, 4th Ed., Marcel Dekker Inc, New York, 1987, 483-496

25 Dodd, J.W. and Tonge, K.H., *Thermal Methods*, 1987, 5-123

26 Anasys thermal methods consultancy, http://www.anasys.co.uk/library/dsc2.htm

27 Newkome, T., *J. Org. Chem.*, 1979, **44**, 1362

28 Morrison, R.T. and Boyd, R.N., *Organic Chemistry*, 5th Ed., Allyn and Bacon Inc, Boston, 1987, 535-934

29 Crocke, H.P. and Walser, R., *J. Chem. Soc. C*, 1970, 1982-1986

30 Dagani, B., *Anal. Biochem.*, 1978, **87**, 455

31 Butler, R.N.,O'Shea, P.D. and Declan, P., *J. Chem. Soc. (London) Perkin Trans. I*, 1987, 1039-1042

32 Anasys thermal methods consultancy, http://www.anasys.co.uk/library/tga2.htm

33 Petrucci, R.H., *General Chemistry*, 5th Ed., Macmillan Publishing Co., New York, 1989, 410-414

34 Carey, F.A. and Richard, J.S., *Advanced Organic Chemistry Part A: Structure and Mechanisms*, 3rd Ed., Plenum Press, New York, 1990, 222

35 http://www.iupac.org/goldbook/V06597.pdf

36 Bruice, P.Y., *Organic Chemistry*, 3rd Ed, Prentice Hall, New Jersey, 2000, 518

37 Banwell, C.N. and McCash, E.M., *Fundamental of Molecular Spectroscopy*, 4rth Ed., McGraw-Hill, London, 1994, 112

38 Solomons, T.W.J., *Organic Chemistry*, 5th Ed., John Wiley and Sons Inc., New York, 1992, 558-560

39 Zerbi, G. and Sandroni, S., *Spectrochim. Acta A*, 1968, **24**, 483-510

40 Burton, W.R. and Richards R.E., *J. Chem. Soc.*, 1950, 1316-1318

41 Josien, M.L., *Bull. Soc. Chim. Fr.*, 1956, 53

42 Katritzky, A.R. and Lagowski, J.M., *J. Chem. Soc.*, 1958, 4155

43 Akyuz, S., *Vib. Spectr.*, 1997, **14**, 151-154

44 Konings, Ir.J., *Tabellen voor het gecombineerd interpreteren van UV, IR, NMR en MS spectra*, TU Eindhoven, june 1987, 25

45 Hargreaves, A. and Rizvi, S.H., *Acta Cryst.*, 1962, **15**, 365

46 Trotter, J., *Acta Cryst.*, 1961, **14**, 1135

47 Hoffmann, R.A. and. Kinell, P.O., *Arch. Sci. (Geneva)*, 1958, **11**, 228

48 Hadzi, D. and Skrbljak (Miss), *J. Chem. Soc.*, 1957, 843

49 Andreev, G.N., Stamboliyska, B.A. and Penchev, P.N., *Spectrochim. Acta A*, 1977, **53**, 811-818

50 James, R.W. and Saunder, D.H., *Acta Cryst.*, 1948, **1**, 81-83

51 http://www.ccdc.cam.ac.uk/products/csd/

52 Nakai, H., Saito, T. and Yamakawa, M., *Acta Cryst.*, 1988, **C44**, 2117

53 Brock, C.P. and Haller, K.L., *J. Phys. Chem.*, 1984, **88**, 3570

54 Charbonneau, G.P. and Delugeard, Y., *Acta Cryst.*, 1977, **B33**, 1586

55 Brock, C.P., *Acta Cryst.*, 1980, **B36**, 968-971

56 Jackish, M.A., Fronczek, F.R., Geiger, C.C., Hale, P.S., Daly, W.H. and Butler, L.G, *Acta Cryst.*, 1990, **C46**, 919

57 Brock, C.P. and Haller, K.L., *Acta Cryst.*, 1984, **C40**, 1387

58 Atwood, J.L., Davies, J.E.D., MacNicol, D.D. and Vögtle, F., *Comprehensive Supramolecular Chemistry*, Pergamon, Oxford, 1996, **9**

59 Philp, D. and Stoddart, J.F., *Angew. Chem. Int. Ed. Engl.*, 1996, **35**, 1154

60 http://nanonet.rice.edu/research/CVtutorial2/img004.gif

61 http://www-biol.paisley.ac.uk/marco/Enzyme_Electrode/Chapter1/Cyclic_Voltammetry1.htm